A New Entry into Molybdenum/Tungsten Sulfur Chemistry: Synthesis and Reactions of Mononuclear Sulfido Complexes of Pentamethylcyclopentadienyl−Molybdenum(VI) and −Tungsten(VI)

Hiroyuki Kawaguchi, Kazuhiro Yamada, Jian-Ping Lang, and Kazuyuki Tatsumi*

Contribution from the Department of Chemistry, Graduate School of Science, Nagoya University, Furo-cho, Chikusa-ku, Nagoya 464-01, Japan

Received May 27, 1997[⊗]

Abstract: A series of mononuclear thio complexes of pentamethylcyclopentadienyl−molybdenum(VI) and −tungsten-(VI) have been synthesized via C−S bond-cleaving reactions of thiolates. Use of Li_2S_2 for sulfurization of Cp^*MoCl_4 resulted in the known dinuclear complex, *anti*-$Cp^*_2Mo_2(S)_2(\mu\text{-}S)_2$ (**1**), while the analogous reaction of Cp^*WCl_4 gave rise to *anti*-$Cp^*_2W_2(S)_2(\mu\text{-}S)_2$ (**2**) and $(PPh_4)[Cp^*W(S)_3]$ (**3**), the latter of which was isolated after the subsequent cation exchange reaction with PPh_4Br. In contrast, the reaction of Cp^*WCl_4 with Li_2edt (edt = SCH_2CH_2S) followed by treatment with PPh_4Br generated **3** as the sole isolable product in high yield. A similar reaction between Cp^*WCl_4 and LiS^tBu afforded $Cp^*W(S)_2(S^tBu)$ (**6**), which turned out to be thermally unstable in solution and gradually degraded to **2**. In these reactions of Cp^*WCl_4 with lithium thiolates, a facile C−S bond cleavage took place and the tungsten atom was oxidized from W(V) to W(VI). On the other hand, the Mo(IV) thiolate complexes, $Cp^*Mo(S^tBu)_3$ (**4**) and $(PPh_4)[Cp^*Mo(edt)_2]$ (**5**), were formed from the Cp^*MoCl_4/LiS^tBu and Cp^*MoCl_4/Li_2edt/PPh_4Br reaction systems. The complex **4** was readily oxidized by dry O_2 producing $Cp^*Mo(O)_2(S^tBu)$ (**7**) exclusively, while the reactions of **4** with NH_2NMe_2 and NH_2NHPh occurred slowly to yield $Cp^*Mo(S)_2(S^tBu)$ (**8**). The hydrazines acted as oxidants, presumably by cleaving the N−N bond, and promoted the C−S bond rupture of *tert*-butyl thiolate and concomitant oxidation of molybdenum from Mo(IV) to Mo(VI). Elemental sulfur S_8 and grey selenium also acted as oxidants in the reactions with **4**, leading to a complex mixture of products. From the **4** + S_8 reaction, the complexes **1**, **8**, and $Cp^*Mo(O)(S)(S^tBu)$ (**9**) were produced, and the **4** + Se reaction lead to **8** and *anti*-$Cp^*_2Mo_2(E)_2(\mu\text{-}E)_2$ (**10**; E = S, Se). Finally treatment of **8** with Li_2S_2 and PPh_4Br afforded $(PPh_4)[Cp^*Mo(S)_3]$ (**11**). We found that **11** was synthesized more easily by a one-pot reaction of **4**, $^1/_4$ equiv of S_8, and Li_2S_2 in THF. The trithio complexes, **3** and **11**, reacted very cleanly with PhC≡CPh generating $(PPh_4)[Cp^*M(S)(S_2C_2Ph_2)]$ (M = W (**12**), Mo (**13**)), respectively. A kinetic study of these reactions showed that they were first order in PhC≡CPh and first order in **3** or **11** with appreciable negative entropies of activation and that the activation barrier was higher for the molybdenum reaction. The crystal structures of **3**−**8** and **11**−**13** were determined by the X-ray analysis.

Introduction

The importance of group 6 transition metal sulfides in metalloenzymes as well as in industrial processes, such as hydrodesulfurization and electro/photocatalysis, is well documented.[1,2] A wide variety of sulfur-ligated complexes of molybdenum and tungsten have been synthesized, providing a diverse range of structural features.[3] However, aside from tetrathiometallates $[M(S)_4]^{n-}$ and their derivatives,[4] compounds containing the terminal thio ligand (S^{2-}) with M═S multiple bonding are less common compared with the ubiquitous oxo complexes.[5] Even more scarce are mononuclear thio complexes having two or three M═S bonds.[5b,f,g] This is due to lack of an appropriate synthetic route to such thio complexes, where difficulty arises from the following three reasons. First, sulfur ligands have a propensity for bridging metal atoms, leading to multinuclear sulfide compounds. Second, metal sulfides are thought to undergo disproportionation reactions in solution, via intramolecular electron transfer processes, resulting in S−S bond formation and concomitant reduction of metal centers. For instance, $[M(S)_4]^{2-}$ (M = Mo(VI), W(VI)) are readily transformed to various polythiomolybdate and polythiotungstate anions.[6] Third, reaction of thio ligands with transition metals is often carried out under reducing conditions which facilitates metal−metal bond formation, because sulfurization reagents such as alkali metal sulfides and alkaline earth metal sulfides act as strong bases. Thus, synthesis of mononuclear thio complexes of molybdenum and tungsten remains a challenging subject. Interestingly, mononuclear molybdenum and tungsten mono-thio complexes have been isolated by Enemark and Young using a bulky tris(pyrazolyl)borate auxiliary ligand.[7] On the

[⊗] Abstract published in *Advance ACS Abstracts,* October 15, 1997.

(1) Stiefel, E. I.; Coucouvanis, D.; Newton, W. E. *Molybdenum Enzymes, Cofactors, and Model Systems*; American Chemical Society: Washington, DC, 1993.

(2) Stiefel, E. I.; Matsumoto, K. *Transition Metal Sulfur Chemistry, Biological and Industrial Significance*; American Chemical Society; Washington, DC, 1996.

(3) Braithwaite, E. R.; Haber, J. *Molybdenum: An Outline of its Chemistry and Uses*; Elsevier Science B. V.: Amsterdam, 1994.

(4) Müller, A.; Diemann, E.; Jostes, R.; Bögge, H. *Angew. Chem., Int. Ed. Engl.* **1981**, *20*, 934−955.

(5) (a) Trnka, T. M.; Parkin, G. *Polyhedron* **1997**, *16*, 1031−1045. (b) Murphy, V. J.; Parkin, G. *J. Am. Chem. Soc.* **1995**, *117*, 3522−3528. (c) Rabinovich, D.; Parkin, G. *Inorg. Chem.* **1995**, *34*, 6341−6361. (d) Rice, D. *Coord. Chem. Rev.* **1978**, *25*, 199−227. (e) Vahrenkamp, H. *Angew. Chem., Int. Ed. Engl.* **1975**, *14*, 322−329. (f) Cotton, F. A.; Schmid, G. *Inorg. Chem.* **1997**, *36*, 2267−2278. (g) Faller, J. W.; Kucharczyk, R. R.; Ma, Y. *Inorg. Chem.* **1990**, *29*, 1662−1667.

(6) Hadjikyriacou, A. I.; Coucouvanis, D. *Inorg. Chem.* **1987**, *26*, 2400−2408.

(7) (a) Enemark, J. H.; Young, C. G. *Adv. Inorg. Chem.* **1993**, *40*, 1−88. (b) Young, C. G.; Roberts, S. A.; Ortega, R. B.; Enemark, J. H. *J. Am. Chem. Soc.* **1987**, *109*, 2938−2946. (c) Young, C. G.; Enemark, J. H.; Collison, D.; Mabbs, F. E. *Inorg. Chem.* **1987**, *26*, 2925−2927.

S0002-7863(97)01725-3 CCC: $14.00

other hand, there are numerous binuclear thio complexes which contain a cyclopentadienyl ligand, e.g., $Cp^*_2M_2(S)_2(\mu\text{-}S)_2$, $Cp^*_2M_2(S)_2(\mu\text{-}S_2)$, and $Cp^*_2M_2(S)(\mu\text{-}S)_2(CO)_2$ (M = Mo, W).[8]

Considering the favorable match, both in spatial extension and in energy, between the S 3p and Mo 4d (and W 5d) orbitals, we sense that the M═S bond is thermodynamically stable once it is formed, if the metal atom has vacant d_π orbitals. Thus a key to the synthesis of thio complexes would be to attain and/or to retain a high oxidation state of metal centers during the sulfurization reaction. From this point of view, reductive C−S bond cleavage of thiolates may be a useful method for generation of M═S bonds.[9] On the basis of this strategy, we have developed chemistry of a new family of mononuclear thio complexes of pentamethylcyclopentadienyl−molybdenum and −tungsten, the results of which are described in this paper with the emphasis on the successful isolation of trithio complex anions, $[Cp^*Mo(S)_3]^-$ and $[Cp^*W(S)_3]^-$. Also reported herein are an addition reaction of diphenylacetylene to the terminal sulfides of the trithio complexes and its kinetic study. A short communication of the high-yield synthesis of $[Cp^*W(S)_3]^-$ has been published.[10]

An impetus for this study was the isolation of the first organometallic trithio complexes of group 5 metals, $[Cp^*M(S)_3Li_2(THF)_2]_2$ (M = Nb, Ta).[11] We synthesized these complexes from Cp^*MCl_4 and Li_2S_2 and demonstrated that the lithium cations were readily replaced by late transition metals, giving rise to heterometallic sulfido clusters.[12] Preparation of the tetrathiometallates of Nb(V) and Ta(V) were reported slightly earlier than our synthesis of the above trithio complexes.[13] The electronic and structural similarity between $[M(S)_4]^{3-}$, $[Cp^*M(S)_3]^{2-}$ (M = Nb, Ta), and $[M(S)_4]^{2-}$, $[Cp^*M(S)_3]^-$ (M = Mo, W) prompted us to examine the chemistry of the half-sandwich thio complexes of Mo(VI) and W(VI) (Chart 1). The related oxo complexes, $[Cp^*Mo(O)_3]^-$ and $[Cp^*W(O)_3]^-$ have been reported.[14]

Chart 1

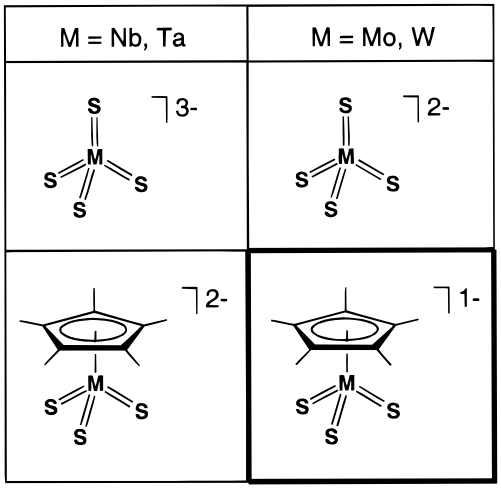

Experimental Section

General Procedures. All reactions and the manipulations of air-sensitive compounds were performed under an inert atmosphere using standard Schlenk and glovebox techniques. Solvents were dried, degassed, and distilled from sodium/benzophenone ketyl (THF, toluene, hexane) or from CaH_2 (CH_3CN) under argon.

^{1}H NMR spectra were recorded on JEOL GSX-270 and Varian UNITYplus-500 spectrometers, and chemical shifts are quoted in ppm relative to the signals of deuterated solvents. All spectra were acquired at room temperature unless otherwise noted. Deuterated solvents were vacuum-transferred from sodium (benzene-d_6) or CaH_2 ($CDCl_3$, CD_3CN). DMF-d_7 was stored over 4-Å molecular sieves. For UV−visible spectra, JASCO V-560 and U-best-30 spectrometers were used. Infrared spectra were recorded on a Parkin Elmer 2000 FT-IR spectrometer. Mass spectra were collected on either a Shimadzu QP5000 mass spectrometer or a Perkin-Elmer API 300 mass spectrometer. Elemental analyses were performed on a LECO-CHN and LECO-CHNS microanalyzers where the crystalline samples were sealed in thin aluminum and tin tubes.

Cp^*MoCl_4 and Cp^*WCl_4 were synthesized according to literature procedures.[15] Li_2S_2 and Li_2S were prepared in liquid NH_3 as described previously,[11a] and the yellow and white solids obtained therefrom were washed with THF before use. NH_2NMe_2 and NH_2NHPh were distilled from CaH_2 and stored over 4-Å sieves. LiS^tBu and Li_2edt were prepared from the reactions of HS^tBu and H_2edt with *n*-C_4H_9Li (1.6 M hexane solution) in THF at 0 °C just prior to use. Elemental sulfur (S_8) was recrystallized from toluene, and selenium purchased from Wako was used as received.

Reaction of Cp^*MoCl_4 with Li_2S_2. To a THF (20 mL) slurry of Li_2S_2 (0.39 g, 5.0 mmol) was added Cp^*MoCl_4 (0.28 g, 0.75 mmol) in THF (20 mL) at 0 °C, resulting in a brown suspension. The solution was stirred at room temperature for 1 h and was then evaporated to dryness. The residue was extracted with toluene (50 mL) and centrifuged. The solvent was removed *in vacuo* from the extract to yield a brown crystalline solid. Recrystallization from THF/hexane afforded *anti*-$Cp^*_2Mo_2(S)_2(\mu\text{-}S)_2$ (**1**) as brown crystals (0.19 g, 88%).[16] ^{1}H NMR ($CDCl_3$): δ 2.06 (s, C_5Me_5). IR (Nujol): 490 (s, $\nu_{Mo=S}$), 447 (m, $\nu_{Mo-S-Mo}$) cm^{-1}. MS (EI): *m/z* 590 (M^+). Anal. Calcd for $C_{20}H_{30}S_4Mo_2$: C, 40.67; H, 5.12. Found: C, 40.78; H, 5.03.

Reaction of Cp^*WCl_4 with Li_2S_2. A mixture of Cp^*WCl_4 (0.57 g, 1.24 mmol) and Li_2S_2 (0.54 g, 6.92 mmol) in THF (70 mL) was stirred at room temperature for 1 h to give a reddish-brown suspension. The solution was evaporated to dryness. The resulting residue was extracted with toluene (50 mL). Removal of the solvent *in vacuo* left a red crystalline solid, and CH_3CN (40 mL) was added to give a red solution and a brown solid. After centrifugation to remove the brown solid, a CH_3CN (10 mL) solution of PPh_4Br (0.50 g, 1.19 mmol) was added to the red supernatant. Concentration of the CH_3CN solution afforded $(PPh_4)[Cp^*W(S)_3]$ (**3**) as orange crystals (0.57 g, 61%). The brown solid insoluble in CH_3CN was recrystallized from toluene/hexane, providing *anti*-$Cp^*_2W_2(S)_2(\mu\text{-}S)_2$ (**2**) as reddish−brown crystals (0.12 g, 25%).[8b,14a]

Data for **2**. ^{1}H NMR ($CDCl_3$): δ 2.26 (s, C_5Me_5). IR (Nujol): 468 (s, $\nu_{W=S}$) 436 (w, ν_{W-S-W}) cm^{-1}. Anal. Calcd for $C_{20}H_{30}S_4W$: C, 31.34; H, 3.95; S, 16.74. Found: C, 31.80; H, 3.89; S, 17.02.

Data for **3**. ^{1}H NMR (DMF-d_7): δ 8.1−7.9 (m, 20H, Ph), 2.10 (s, 15H, C_5Me_5). IR (Nujol): 466 (s, $\nu_{W=S}$), 437 (s, $\nu_{W=S}$) cm^{-1}. UV−

(8) (a) Wachter, J. *Angew. Chem., Int. Ed. Engl.* **1989**, *28*, 1613−1626. (b) Brunner, H.; Meier, W.; Wachter, J. Guggolz, E.; Zahn, T.; Ziegler, M. L. *Oraganometallics* **1982**, *1*, 1107−1113. (c) Rakowski DuBois, M. *Chem. Rev.* **1989**, *89*, 1−9.

(9) Blower, P. J.; Dilworth, J. R.; Hutchinson, J. P.; Zubieta, J. A. *Inorg. Chim. Acta* **1982**, *65*, L225−L226.

(10) Kawaguchi, H.; Tatsumi, K. *J. Am. Chem. Soc.* **1995**, *117*, 3885−3886.

(11) (a) Tatsumi, K.; Inoue, Y.; Kawaguchi, H.; Kohsaka, M.; Nakamura, A.; Cramer, R. E.; VanDoorne, W.; Taogoshi, G. J.; Richmann, P. N. *Organometallics* **1993**, *12*, 352−364. (b) Tatsumi, K.; Inoue, Y.; Nakamura, A.; Cramer, R. E.; VanDoorne, W.; Gilje, J. W. *J. Am. Chem. Soc.* **1989**, *111*, 782−783.

(12) Tatsumi, K.; Kawaguchi, H.; Inoue, Y.; Nakamura, A.; Cramer, R. E.; Golen, J. A. *Angew. Chem., Int. Ed. Engl.* **1993**, *32*, 763−765.

(13) (a) Lee, S. C.; Li, J.; Mitchell, J. C.; Holm, R. H. *Inorg. Chem.* **1992**, *31*, 4333−4338. (b) Lee, S. C.; Holm, R. H. *J. Am. Chem. Soc.* **1990**, *112*, 9654−9655.

(14) (a) Rau, M. S.; Kretz, C. M.; Geoffroy, G. L.; Rheingold, A. L. *Organometallics* **1993**, *12*, 3447−3460. (b) Rau, M. S.; Kretz, C. M.; Mercando, L. A.; Geoffroy, G. L; Rheingold, A. L. *J. Am. Chem. Soc.* **1991**, *113*, 7420−7421.

(15) (a) Liu, A. H.; Murray, R. C.; Dewan, J. C.; Santarsiero, B. D.; Schrock, R. R. *J. Am. Chem. Soc.* **1987**, *109*, 4282−4291. (b) Murray, R. C.; Blum, L.; Liu, A. H.; Schrock, R. R. *Organometallics* **1985**, *4*, 953−954.

(16) Rakowski Dubois, M.; DuBois, D. L.; VanDerveer, M. C.; Haltiwanger, R. C. *Inorg. Chem.* **1981**, *20*, 3064−3071.

visible (λ_{max}, nm (ϵ, $M^{-1}cm^{-1}$), CH_3CN): 268 (20 000), 274 (18 000), 317 (2500), 377 (28 000), 432 (3600). Anal. Calcd for $C_{34}H_{35}S_3PW$: C, 54.11; H, 4.67; S, 12.75; P, 4.10. Found: C, 53.97; H, 4.77; S, 12.55; P, 3.88.

Synthesis of Cp*Mo(S^{t}Bu)$_3$ (4). Addition of LiS^{t}Bu (4.07 mmol) in THF (20 mL) to a THF (10 mL) slurry of Cp*$MoCl_4$ (0.38 g, 1.02 mmol) at 0 °C formed a dark-red homogeneous solution. The mixture was stirred at room temperature for 1 h, and removal of the solvent left a dark red residue. The residue was extracted with hexane (50 mL) and centrifuged to remove LiCl. The supernatant was concentrated under vacuum to yield 0.43 g of **4** as dark red crystals (85%). ^{1}H NMR (C_6D_6): δ 1.82 (s, 27H, SC*Me*$_3$), 1.75 (s, 15H, C_5*Me*$_5$). IR (Nujol): 1335 (s), 1155 (s), 1020 (s) cm^{-1}. UV−visible (λ_{max}, nm (ϵ, M^{-1} cm^{-1}), hexane): 481 (640), 593 (490). MS (EI): *m/z* 329 ($M^+ - 3C_4H_9$). Anal. Calcd for $C_{22}H_{42}S_3Mo$: C, 52.98; H, 8.49. Found: C, 52.93; H, 8.51.

Synthesis of (PPh$_4$)[Cp*Mo(edt)$_2$] (5). To a slurry of Li_2edt (4.50 mmol) in THF (30 mL) was added Cp*$MoCl_4$ (0.67 g, 1.80 mmol) in THF (20 mL) at 0 °C. This immediately produced a red homogeneous solution, which was warmed to room temperature and stirred for 1 h. After removal of the solvent *in vacuo*, the red residue was extracted with 60 mL of CH_3CN. The CH_3CN solution was centrifuged to remove insoluble LiCl, and PPh_4Br (0.75 g, 1.80 mmol) in CH_3CN (20 mL) was added to the supernatant. The solution was concentrated to afford **5**·CH_3CN as red crystals (1.19 g, 88% yield). ^{1}H NMR ($CDCl_3$): δ 7.5 − 7.9 (m, 20H, PPh_4), 2.8 (s, br, 8H, $S_2C_2H_4$), 1.99 (s, 3H, C*H*$_3$CN), 1.84 (s, br, 15H, C_5*Me*$_5$). IR (Nujol): 1108 (s), 1010 (m), 996 (m), 758 (m), 721 (s), 690 (m), 532 (s), 461 (w) cm^{-1}. UV−visible (λ_{max}, nm (ϵ, M^{-1} cm^{-1}), CH_3CN): 387 (1700), 457 (3500). Anal. Calcd for $C_{40}H_{46}MoNPS_4$: C, 60.36; H, 5.82; N, 1.76; P, 3.89; S, 16.11. Found: C, 60.19; H, 5.99; N, 1.57; P, 4.01; S, 16.00.

Reaction of Cp*WCl_4 with LiS^{t}Bu. A THF (20 mL) solution of LiS^{t}Bu (2.2 mmol) was added to Cp*WCl_4 (0.25 g, 0.54 mmol) in THF (20 mL) at 0 °C. The reaction mixture immediately became a homogeneous red solution and was stirred for 1 h at room temperature. The solvent was removed *in vacuo*. The resulting solid was extracted with hexane (40 mL) and centrifuged to give a red solution and a brown solid. Concentration of the red solution resulted in precipitation of Cp*W(S)$_2$(S^{t}Bu) (**6**) as red crystals (0.10 g, 38%). The brown solid insoluble in hexane was treated with toluene to give *anti*-Cp*$_2$W$_2$(S)$_2$-(μ-S)$_2$ (**2**) (42 mg, 20% based on W). ^{1}H NMR ($CDCl_3$): δ 2.26 (s, 15H, C_5*Me*$_5$), 1.55 (s, 9H, SC*Me*$_3$). IR (Nujol): 1148 (s), 1028 (m), 800 (w), 719 (w), 552 (w), 488 (s, $\nu_{W=S}$), 479 (s, $\nu_{W=S}$) cm^{-1}. UV−visible (λ_{max}, nm (ϵ, M^{-1} cm^{-1}), THF): 289 (6100), 376 (7400), 420 (sh). Anal. Calcd for $C_{14}H_{24}S_3W$: C, 35.60; H, 5.12. Found: C, 35.57; H, 5.12.

When the reaction mixture of Cp*WCl_4 (0.16 g, 0.35 mmol) and LiS^{t}Bu (1.4 mmol) in THF (30 mL) was stirred for 12 h at room temperature, the color of the solution changed from red to brown. The solution was then evaporated to dryness. The residue was extracted with toluene (60 mL) and centrifuged to remove LiCl. Concentration of the brown toluene solution gave *anti*-Cp*$_2$W$_2$ (S)$_2$(μ-S)$_2$ (**2**) as brown crystals (75 mg, 58%).

Reaction of Cp*WCl_4 with Li_2edt. To a THF (30 mL) suspension of Li_2edt (5.30 mmol) was added Cp*WCl_4 (1.22 g, 2.65 mmol) in THF (30 mL) at 0 °C, immediately producing an orange-red homogeneous solution. After 2 h of stirring at room temperature, the solution was evaporated under vacuum to dryness. The red residue was extracted with warm CH_3CN (60 mL) and centrifuged to remove an insoluble material. A CH_3CN (30 mL) solution of PPh_4Br (1.05 g, 2.51 mmol) was added to the extract, and concentration of the solution gave an orange solid. Recrystallization from warm CH_3CN afforded orange crystals (1.64 g, 82% yield), which were identified as **3** according to the spectroscopic data and elemental analyses.

Thermodecomposition of (PPh$_4$)[Cp*Mo(edt)$_2$]. A DMF (40 mL) solution of (PPh$_4$)[Cp*Mo(edt)$_2$] (**5**) (0.77 g, 0.97 mmol) was stirred at 140 °C for 4 h. The color of the solution gradually changed from dark red to brown. After the solvent was removed *in vacuo*, the residue was extracted with THF to leave a brown solid. Concentration of the THF solution gave Cp*$_2$Mo$_2$(S)$_2$(μ-S)$_2$ (**1**) (66 mg, 23% based on Mo). The brown solid insoluble in THF was recrystalllized from CH_3CN to yield (PPh$_4$)$_2$[Mo(S)$_4$] (0.23 g, 26%). These compounds were identified by spectroscopic data and elemental analyses.

Reaction of 4 with O_2. A THF (30 mL) solution of **4** (0.45 g, 0.91 mmol) was stirred under a dry O_2 atmosphere (1 atm) at room temperature, and the solution quickly turned green. After being stirred for 10 h, the solvent was removed *in vacuo*. The green residue was dissolved in a minimum amount of hexane, and the solution was cooled to −20 °C. Yellow crystals of Cp*Mo(O)$_2$(S^{t}Bu) (**7**) were obtained (0.27 g, 83%). ^{1}H NMR (C_6D_6): δ 1.72 (s, 15H, C_5*Me*$_5$), 1.62 (s, 9H, SC*Me*$_3$). IR (Nujol): 1378 (s), 1160 (s), 1035 (s), 901 (s, $\nu_{Mo=O}$), 875 (s, $\nu_{Mo=O}$) cm^{-1}. UV−visible (λ_{max}, nm (ϵ, M^{-1} cm^{-1}), hexane): 270 (9800), 330 (21400). MS (EI): *m/z* 297 ($M^+ - C_4H_9$). Anal. Calcd for $C_{14}H_{24}O_2SMo$: C, 47.72; H, 6.87. Found: C, 48.06; H, 7.13.

Reaction of 4 with NH_2NMe_2 and NH_2NHPh. To a THF (20 mL) solution of **4** (0.39 g, 0.79 mmol) was added NH_2NMe_2 (0.24 mL, 3.1mmol). The dark-red solution was stirred at room temperature. After the disappearance of the red color in 3 days, the solution was evaporated to dryness. The resulting brown residue was extracted with hexane (40 mL) and centrifuged to remove insoluble material. Concentration and cooling of the extract to −20 °C produced Cp*Mo(S)$_2$(S^{t}Bu) (**8**) as brown crystals (0.11 g, 35%). ^{1}H NMR (C_6D_6): δ 1.73 (s, 15H, C_5*Me*$_5$), 1.65 (s, 9H, SC*Me*$_3$). IR (Nujol): 1370 (s), 1355 (s), 1150 (s), 1020 (s), 485 (s, $\nu_{Mo=S}$) cm^{-1}. UV−visible (λ_{max}, nm (ϵ, M^{-1} cm^{-1}), hexane): 342 (9200), 439 (11 000), 470 (sh). MS (EI): *m/z* 329 ($M^+ - C_4H_9$). Anal. Calcd for $C_{14}H_{24}S_3Mo$: C, 43.74; H, 6.29. Found: C, 43.52; H, 6.15.

A THF (20 mL) solution of **4** (0.28 g, 0.56 mmol) was treated with NH_2NHPh (0.22 mL, 2.2 mmol), and a workup similar to the one described above afforded 88 mg of **8** in 41% yield.

Reaction of 4 with S_8. Compound **4** (0.58 g, 1.2 mmol) and S_8 (74 mg, 0.29 mmol) were placed in a flask and dissolved in 50 mL of THF. The mixture was stirred at room temperature for 8 h, during which time the color of the solution gradually changed from dark-red to green. After removal of the volatiles, the residue was extracted with hexane to leave a brown solid. Recrystallization of the brown solid from toluene gave *anti*-Cp*$_2$Mo$_2$(S)$_2$(μ-S)$_2$ (**1**) as brown crystals (20 mg, 12% based on Mo). Concentration and cooling the extract to −20 °C gave red crystals (0.10 g) and green crystals (0.17 g), which were separated manually. The red compound was the mixture of Cp*Mo-(S)$_2$(S^{t}Bu) (**8**) and Cp*Mo(O)(S)(S^{t}Bu) (**9**).

Data for the mixture of **8** and **9**. ^{1}H NMR (C_6D_6): δ 1.73 (s, C_5*Me*$_5$, **8**), 1.70 (s, C_5*Me*$_5$, **9**), 1.65 (s, SC*Me*$_3$, **8**), 1.61 (s, SC*Me*$_3$, **9**). IR (Nujol): 1370 (s), 1355 (s), 1150 (s), 1020 (s), 890 (s, $\nu_{Mo=O}$), 485 (s, $\nu_{Mo=S}$) cm^{-1}. MS (EI): *m/z* 329 ([Cp*MoS_3]$^+$), 313 ([Cp*MoS_2O]$^+$). Crystal data for the mixture of **8** and **9**: orthorhombic, space group *Pnma* with a = 8.514(2) Å, b =12.041(3) Å, c = 16.421(4) Å, V = 1683.5(7) Å^3, and Z = 4. The structure analysis revealed the positions of Cp*, Mo, and S^{t}Bu unequivocally with a crystallographic mirror plane through the molecule. A strong peak appeared in the vicinity of Mo, which could be assigned to a terminal sulfide. However, the Mo peak distance of 2.021(5) Å is obviously too short for an Mo═S bond, and inspection of thermal and occupancy parameters suggested that the crystal was compositionally disordered between **8** and **9**.

Reaction of 4 with Selenium. The mixture of **4** (0.25 g, 0.50 mmol) and grey selenium (78 mg, 0.99 mmol) in THF (20 mL) was stirred for 12 h at room temperature. The color of the solution gradually changed from dark red to brown. After removal of the solvent *in vacuo*, Cp*Mo(S)$_2$(S^{t}Bu) (**8**) (62 mg, 33%) was extracted from the brown residue by hexane. The red solid insoluble in hexane was recrystallized from toluene, giving purple crystalline Cp*$_2$Mo$_2$(E)$_2$(μ-E)$_2$ (E = S, Se) (**10**) (0.11 g). Data for **10**: ^{1}H NMR (C_6D_6): δ 2.12 (s, C_5*Me*$_5$), 2.09 (s, C_5*Me*$_5$). IR (Nujol): 485 (s, $\nu_{W=S}$) cm^{-1}. UV−visible (λ_{max}, nm, toluene): 489, 347, 293. Crystal data for **10**: orthorhombic, space group $P2_1/n$ with a = 7.907(1) Å, b = 15.252(3) Å, c = 10.124(1) Å, β = 104.92(1)°, V = 1179.9(4) Å^3, and Z = 2.

Synthesis of (PPh$_4$)[Cp*Mo(S)$_3$] (11). Method A. A Schlenk tube was charged with **4** (1.27 g, 2.55 mmol) and S_8 (0.16 g, 0.62 mmol) in a glovebox. The Schlenk tube was taken out of the box, and THF (30 mL) was added. The solution was stirred at room temperature for 12 h, during which time the color turned green. The resulting green

Table 1. Crystal Data for $(PPh_4)[Cp^*M(S)_3]$ (M = W (**3**), Mo (**11**)), $Cp^*Mo(S^tBu)_3$ (**4**), $(PPh_4)[Cp^*Mo(SCH_2CH_2S)_2]$ (**5**), $Cp^*W(S)_2(S^tBu)$ (**6**), $Cp^*Mo(E)_2(S^tBu)$ (E = O (**7**), S (**8**)), and $(PPh_4)[Cp^*M(S)(S_2C_2Ph_2)]$ (M = W (**12**), Mo (**13**))

	3	**4**	**5**	**6**	**7**	**8**	**11**	**12**	**13**
formula	$C_{34}H_{35}S_3PW$	$C_{22}H_{42}S_3Mo$	$C_{40}H_{46}NS_4PMo$	$C_{14}H_{24}S_3W$	$C_{14}H_{24}O_2SMo$	$C_{14}H_{24}S_3Mo$	$C_{34}H_{35}S_3PMo$	$C_{52}H_{53}OS_3PW$	$C_{52}H_{55}O_2S_3PMo$
mol wt (g mol^{-1})	754.65	498.69	795.96	472.36	352.33	384.46	666.74	1005.01	935.10
cryst system	orthorhombic	triclinic	monoclinic	orthorhombic	orthorhombic	orhorhombic	orthorhombic	monoclinic	monoclinic
space group	*Pbca* (No. 61)	$P\bar{1}$ (No. 2)	$P2_1/n$ (No. 14)	*Pnma* (No. 62)	*Pnma* (No. 62)	*Pnma* (No. 62)	*Pbca* (No. 61)	$P2_1/n$ (No. 14)	$P2_1/n$ (No. 14)
color of crystal	orange	dark red	red	red	yellow	brown	red	green	brown
a (Å)	18.070(4)	9.309(1)	16.787(2)	8.471(8)	9.232(4)	8.476(2)	18.046(8)	13.221(6)	13.140(2)
b (Å)	20.181(5)	16.273(6)	12.255(2)	12.141(8)	12.125(2)	12.116(2)	20.225(7)	27.83(1)	28.531(7)
c (Å)	17.482(5)	9.2785(8)	18.950(3)	16.670(6)	14.439(2)	16.627(3)	17.051(6)	13.456(4)	13.292(3)
α (deg)		92.04(2)							
β (deg)		107.414(9)	98.38(1)					104.47(3)	102.84(2)
γ (deg)		103.93(2)							
V (Å^3)	6374(2)	1292.9(5)	3856.9(8)	1714(2)	1616.1(5)	1707.6(9)	6387(3)	4793(3)	4858(1)
Z	8	2	4	4	4	4	8	4	4
residuals	$R = 0.038^a$	$R = 0.026^a$	$R = 0.038^a$	$R1 = 0.025^c$	$R1 = 0.036^c$	$R = 0.034^a$	$R = 0.061^a$	$R = 0.034^a$	$R = 0.050^a$
	$R_w = 0.039^b$	$R_w = 0.031^b$	$R_w = 0.042^b$	$wR2 = 0.062^d$	$wR2 = 0.076^d$	$Rw = 0.046^b$	$Rw = 0.062^b$	$Rw = 0.040^b$	$Rw = 0.057^b$
GOF	2.23^e	2.18^e	2.62^e	1.11^f	1.09^f	2.86^e	1.99^e	1.91^f	1.90^e

^{a} $R = \sum||F_o| - |F_c||/\sum|F_o|$. ^{b} $R_w = [\{\sum w(|F_o| - |F_c|)^2\}/\sum wF_o^2]^{1/2}$. ^{c} $R1 = \sum||F_o| - |F_c||/\sum|F_o|$. ^{d} $wR2 = [\{\sum w(F_o^2 - F_c^2)^2\}/\sum w(F_o^2)^2]^{1/2}$. ^{e} GOF $= [\{\sum w(|F_o| - |F_c|)^2\}/(N_o - N_p)]^{1/2}$, where N_o and N_p denote the number of data and parameters. ^{f} GOF $= [\sum w(|F_o^2| - |F_c^2|)^2/(N_o - N_p)]^{1/2}$.

solution was added to Li_2S_2 (1.02 g, 13.1 mmol) in THF (30 mL), and the mixture was stirred at room temperature for 24 h. The color of the solution gradually changed from green to red. After the mixture was centrifuged to remove the insoluble material, the solution was evaporated to dryness. The residue was extracted with CH_3CN (40 mL) and centrifuged again [to remove a brown solid containing *anti*-$Cp^*_2Mo_2(S)_2(\mu\text{-}S)_2$ (**1**), which was recrytsallized from toluene (0.19 g, 25%)], and a CH_3CN solution (20 mL) of PPh_4Br (0.65 g, 1.7 mmol) was added. The solution was concentrated *in vacuo* to afford **11** as red crystals (0.86 g, 51% yield). ^{1}H NMR (DMF-d_7): δ 8.1−7.9 (m, 20H, Ph), 1.86 (s, 15H, C_5Me_5). IR (Nujol): 1585 (m), 1435 (s), 1370 (m), 1110 (s), 1030 (m), 1000 (m), 760 (m), 730 (s), 700 (s), 530 (s), 455 (sh, $\nu_{Mo=S}$), 445 (s, $\nu_{Mo=S}$) cm^{-1}. UV−visible (λ_{max}, nm (ϵ, M^{-1} cm^{-1}), CH_3CN): 268 (15 000), 275 (14 000), 308 (9300), 446 (16 000), 516 (2500). Anal. Calcd for $C_{34}H_{35}S_3PMo$: C, 61.25; H, 5.29; S, 14.43. Found: C, 61.49; H, 4.99; S, 10.57.

Method B. A THF (30 mL) solution of **4** (0.37 g, 0.74 mmol) containing NH_2NMe_2 (0.22 mL, 2.9 mmol) was stirred at room temperature for 4 days, and the volatile materials were removed *in vacuo*. The resulting material was redissolved in 20 mL of THF and was added to a slurry of Li_2S_2 (0.73 g, 9.5 mmol) in THF (25 mL). The mixture was stirred at room temperature for 5 h to give a red suspension. Workup similar to that in Method A, using 0.25 g of PPh_4Br (0.59 mmol), yielded **11** (0.16 g, 32%).

Reaction of $Cp^*Mo(S)_2(S^tBu)$ (8) with Li_2S_2. Addition of a THF (10 mL) solution of **8** (0.16 g, 0.42 mmol) to Li_2S_2 (0.17 g, 2.2 mmol) in THF (10 mL) gave a red suspension. The mixture was stirred for 6 h at room temperature. After removal of THF, the residue was extracted with toluene (20 mL). The red toluene solution was evaporated under vacuum to leave a red solid. The resulting solid was dissolved in 20 mL of CH_3CN, and a CH_3CN (10 mL) solution of PPh_4Br (0.13 g, 0.31 mmol) was added. Concentration and cooling to −20 °C afforded 0.18 g of $(PPh_4)[Cp^*Mo(S)_3]$ (**11**) in 65% yield.

Synthesis of $(PPh_4)[Cp^*M(S)(S_2C_2Ph_2)]$ (M = W (12), Mo(13)). A mixture of **3** (0.13 g, 0.16 mmol) and diphenylacetylene (0.19 g, 0.80 mmol) in 10 mL of CH_3CN was stirred at room temperature for 18 h, during which time the color of the solution gradually changed from orange to green. The resulting solution was evaporated to dryness. The brown residue was dissolved in DME (10 mL) and centrifuged to remove an insoluble solid. Concentration and cooling to −20 °C afforded $(PPh_4)[Cp^*W(S)(S_2C_2Ph_2)]$ (**12**) as yellow green plates (0.14 g, 81%). Data for **12**. ^{1}H NMR (DMF-d_7): δ 8.1−7.9 (m, 20H, Ph), 7.28 (m, 4H, $S_2C_2Ph_2$), 7.11 (m, 4H, $S_2C_2Ph_2$), 6.98 (m, 2H, $S_2C_2Ph_2$), 2.08 (s, 15H, C_5Me_5). IR (Nujol): 1590 (m), 1114 (s), 1075 (m), 1030 (m), 1000 (m), 763 (m), 724 (s), 693 (s), 528 (s), 466 (s, $\nu_{W=S}$) cm^{-1}. Anal. Calcd for $C_{52}H_{53}OS_3PW$: C, 62.15; H, 5.32. Found: C, 62.25; H, 5.35.

A mixture of **11** (31 mg, 46 μmol) and diphenylacetylene (41 mg, 0.23 mmol) in CH_3CN (3 mL) was stirred at room temperature for 12 h to give a brown solution. Workup similar to that above yielded $(PPh_4)[Cp^*Mo(S)(S_2C_2Ph_2)]$ (**13**) as brown plates (26 mg, 61%). Data for **13**. ^{1}H NMR (DMF-d_7): δ 8.1−7.9 (m, 20H, Ph), 7.32 (m, 4H, $S_2C_2Ph_2$), 7.11 (m, 4H, $S_2C_2Ph_2$), 7.02 (m, 2H, $S_2C_2Ph_2$), 1.83 (s, 15H, C_5Me_5). IR (Nujol): 1593 (m), 1437 (m), 1377 (m), 1110 (s), 1026 (m), 998 (m), 764 (m), 726 (s), 692 (s), 528 (s), 469 (s, $\nu_{Mo=S}$) cm^{-1}. Anal. Calcd for $C_{52}H_{53}S_3PMo$: C, 66.79; H, 5.93; S, 10.29. Found: C, 66.25; H, 5.85; S, 10.65.

Kinetic Study of Coupling Reactions between $(PPh_4)[Cp^*M(S)_3]$ (M = Mo, W) and Diphenylacetylene. Kinetic experiments were conducted under pseudo-first-order conditions with the concentration of diphenylacetylene in 10-fold excess or more. The alkyne addition reaction was monitored by ^{1}H NMR spectroscopy over the temperature range 10−35 °C. A representative experiment follows.

An NMR tube was charged with diphenylacetylene (13.3 mg, 0.0747 mmol), and a DMF-d_7 solution (0.70 mL) of **11** (13.1 mg) containing 1,3,5-trimethoxybenzene was added. Plots of ln[**3**] and ln[**11**] versus time were found to be linear for all reactions at 10−35 °C. The resulting pseudo-first-order rate constants, k_{obs}, were divided by the concentration of diphenylacetylene to give second-order rate constants, k_2, L mol^{-1} s^{-1}. The k_2 values obtained at given temperatures are as follows: for **3**, 3.37×10^{-5}, 10 °C; 5.45×10^{-5}, 15 °C; 8.69×10^{-5}, 20 °C; 1.42×10^{-4}, 25 °C; 2.11×10^{-4}, 30 °C; 3.27×10^{-4}, 35 °C; for **11**; 1.70×10^{-3}, 10 °C; 2.44×10^{-3}; 15 °C; 4.14×10^{-3}, 20 °C; 3.96×10^{-3}, 20 °C; 5.28×10^{-3}, 25 °C; 8.78×10^{-3}, 30 °C; 1.17×10^{-2}, 35 °C. Activation parameters were determined from Eyring plots of the above data.

X-ray Crystal Structure Determination. Crystal data, data collection, and refinement parameters for all structurally characterized complexes are summarized in Table 1. Single crystals of **3**, **5**, and **11** were obtained from CH_3CN solutions, while those of **4** and **6**−**8** were obtained from hexane solutions. Crystals of **12** were obtained by the slow diffusion of hexane into a THF solution of the complex, and the slow diffusion of hexane into a DME solution of **13** afforded single crystals. These crystals were mounted in glass capillaries and sealed under argon. Diffraction data were collected at room temperature on a Rigaku AFC7R (for **3**−**5**, **8**, **11**, and **13**) and a Rigaku AFC5R (for **6**, **7**, and **12**) diffractometers employing graphite-monochromatized Mo Kα radiation (λ = 0.710 690 Å) and using the ω−2θ scan technique. Refined cell dimensions and their standard deviations were obtained by least-squares refinements of 25 randomly selected centered reflections. Three standard reflections, monitored periodically for crystal decomposition or movement, showed slight intensity variation over the course of the data collections. The raw intensities were corrected for Lorentz and polarization effects. Empirical absorption corrections based on ψ scans were applied.

Calculations were performed with the TEXSAN package for **3**−**5**, **8**, **11**, and **13**, and with the SHELX76 program for **6** and **12**, and with the SHELX93 program for **7**. The structures of **4**−**6** and **11**−**13** were solved by direct methods, and the other structures were solved by the Patterson method, where the metal atoms and some heavy atoms were located unequivocally. The remaining heavy atoms were found in subsequent Fourier maps, and the structures were refined by block-matrix least-squares for **12** and by full-matrix least-squares for the others. Anisotropic refinement was applied to all non-hydrogen atoms, and all the hydrogen atoms were put at calculated positions. For **5**, both carbons of each edt ligand are disordered with occupancy factors of 50:50. In the case of **12** and **13**, the crystal solvents were refined isotropically, and no hydrogen atom of the DME molecule in **13** was included. Additional data are available as Supporting Information.

Results and Discussion

The readily accessible pentamethylcyclopentadienyl tetrachloro complexes, Cp^*MCl_4 (M = Mo, W)[15] have been chosen as general starting materials for the synthesis of the mononuclear organometallic thio complexes of molybdenum and tungsten described in this paper. The use of the half-sandwich compounds has advantages in that the high oxidation state of the metal center is desirable for the synthesis of thio complexes, and in that the presence of the pentamethylcyclopentadienyl auxiliary ligand promotes solubility of the resulting metal sulfides and its steric bulkiness often avoids complexity arising from cluster formation.

Reactions of Cp^*MCl_4 (M = Mo, W) with Li_2S_2. Taking account of the successful isolation of trithio complexes of niobium and tantalum, $[Cp^*M(S)_3Li_2(THF)_2]_2$ (M = Nb, Ta), from the reaction between d^0 Cp^*MCl_4 and anhydrous Li_2S_2,[11] we first examined the analogous reactions of d^1 Cp^*MoCl_4 and Cp^*WCl_4. Thus we treated Cp^*MoCl_4 with Li_2S_2 in THF. The reaction, however, gave rise to the known dinuclear sulfide complex, *anti*-$Cp^*_2Mo_2(S)_2(\mu\text{-}S)_2$ (**1**),[16] in 88% yield as the sole isolable product, which was characterized by IR, ^{1}H NMR, EI-MS, and elemental analysis. In this reaction, the Mo(V) oxidation state is retained, and the formation of the Mo−Mo bond is not surprising for the d^1 electronic configuration.

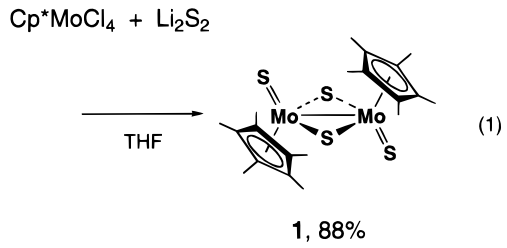

On the other hand, the reaction of Cp^*WCl_4 with Li_2S_2 led to formation of $[Li(THF)_n][Cp^*W(S)_3]$ and *anti*-$Cp^*_2W_2(S)_2(\mu\text{-}S)_2$ (**2**). Fortunately the dinuclear complex **2** is less soluble in CH_3CN than $[Li(THF)_n][Cp^*W(S)_3]$, so the two complexes could be separated by recrystallization. Extraction of the crude product with CH_3CN left a brown solid, recrystallization of which from THF gave analytically pure **2** in 25% yield. Addition of PPh_4Br to the remaining CH_3CN extract and concentration of the solution generated $(PPh_4)[Cp^*W(S)_3]$ (**3**) as orange crystals in 61% yield.

Geoffroy et al. reported that the reaction of Cp^*WCl_4 with H_2S in the presence of NEt_3 produced the trithio complex $(NEt_3H)[Cp^*W(S)_3]$ in low yield along with *anti*-$Cp^*_2W_2(S)_2(\mu\text{-}S)_2$ (**2**), $Cp^*_2W_2(S)_2(S_2)$, and $(NEt_3H)[Cp^*W(S)_2O]$, while the analogous $Cp^*MoCl_4/H_2S/NEt_3$ reaction system gave the dinuclear sulfido complex **1**.[14a] The products obtained from sulfurization of Cp^*MCl_4 (M = Mo, W) by H_2S/NEt_3 bear some resemblance to those from the reactions with Li_2S_2. Although the use of Li_2S_2 is obviously superior to H_2S/NEt_3 in terms of the reduced complexity of the products, the reaction with dilithium 1,2-ethanedithiolate turned out to be a more convenient route to $[Cp^*W(S)_3]^-$, as will be described later in this paper. The X-ray structure analysis of **3** revealed a three-legged piano stool structure with an average W=S distance of 2.192 Å. Since the X-ray structure of $(NEt_3H)[Cp^*W(S)_3]$ was already reported, we refrain from describing it in detail here.

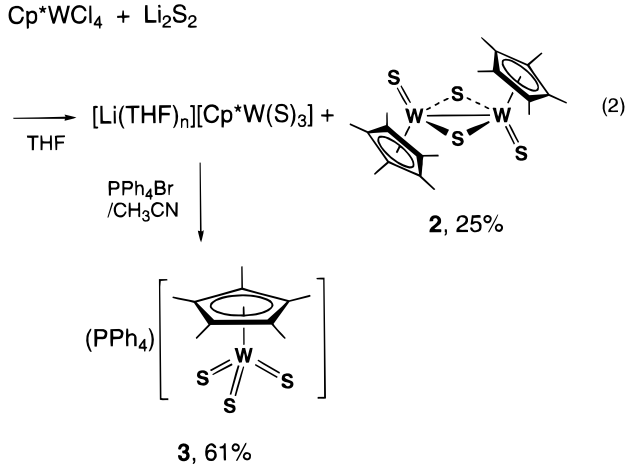

One might argue that Li_2S could be more appropriate than Li_2S_2 as a mono-sulfide (S^{2-}) transfer reagent. However, the reaction between Cp^*WCl_4 and Li_2S produced an inseparable mixture of **2** and ill-defined compound(s), and formation of the desired complex **3** was not discernible. The problem arose probably from the fact that Li_2S is a stronger reductant than Li_2S_2, and thus the oxidation of W(V) to W(VI) in going from Cp^*WCl_4 to **3** is hampered. In fact, as we previously reported, introduction of sulfide into Cp^*TaCl_4 by Li_2S caused a partial reduction of tantalum resulting in the Ta(V)−Ta(IV)−Ta(IV) trinuclear cluster $Cp^*_3Ta_3(S)_6Li_2(THF)_2$, while the analogous reaction with Li_2S_2 gave the Ta(V) sulfide complex $[Cp^*Ta(S)_3Li_2(THF)_2]_2$.[11]

Reactions of Cp^*MoCl_4 with Li^{t}Bu and $Li_2(SCH_2CH_2S)$. The synthesis of mononuclear thio complexes of molybdenum using lithium sulfides failed, and the analogous reactions of tungsten were also not completely satisfactory. At this juncture, we revised our original plan and shifted our investigation to the reactions of Cp^*MCl_4 with Li^{t}Bu and Li_2edt (edt = SCH_2CH_2S). Alkanethiolates have been known to occasionally undergo C−S bond cleavage upon coordination at transition metals, furnishing sulfide/thiolate complexes.[9,17] We previously reported conversion of *tert*-butylthiolate and 1,2-ethanedithiolate into sulfides at Nb(V) and Ta(V) centers[18] and expected that such C−S bond activation might occur for Mo and W complexes as well.

(17) (a) Coucouvanis, D.; Hadjikyriacou, A.; Lester, R.; Kanatzidis, M. G. *Inorg. Chem.* **1994**, *33*, 3645−3655. (b) Coucouvanis, D.; Lester, R. K.; Kanatzidis, M. G.; Kessissoglou, D. P. *J. Am. Chem. Soc.* **1985**, *107*, 8279−8280. (c) Coucouvanis, D.; Hadjikyriacou, A.; Kanatzidis, M. G. *J. Chem. Soc., Chem. Commun.* **1985**, 1224−1225. (d) Coucouvanis, D.; Al-Ahmad, S.; Kim, C. G.; Koo, S.-M. *Inorg. Chem.* **1992**, *31*, 2996−2998. (e) Coucouvanis, D.; Chen, S.-J.; Mandimutsira, B. S.; Kim, C. G. *Inorg. Chem.* **1994**, *33*, 4429−4430. (f) Mandimutsira, B. S.; Chen, S.-J.; Demadis, K. D.; Coucouvanis, D. *Inorg. Chem.* **1995**, *34*, 2267−2268. (g) Seela, J. L.; Huffman, J. C.; Christou, G. *Polyhedron* **1989**, *8*, 1797−1799. (h) Kamata, M.; Yoshida, T.; Otsuka, S.; Hirotsu, K.; Higuchi, T. *J. Am. Chem. Soc.* **1981**, *103*, 3572−3574.

(18) (a) Tatsumi, K.; Sekiguchi, Y.; Nakamura, A.; Cramer, R. E.; Rupp, J. J. *J. Am. Chem. Soc.* **1986**, *108*, 1358−1359. (b) Tatsumi, K.; Kawaguchi, H.; Matsubara, I.; Nakamura, A.; Miki, K.; Kasai, N. *Inorg. Chem.* **1993**, *32*, 2604−2606. (c) Tatsumi, K.; Tahara, A.; Nakamura, A. *J. Organomet. Chem.* **1994**, *471*, 111−115.

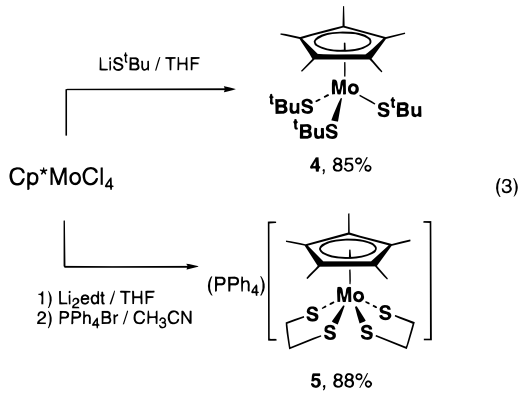

Addition of 4 equiv of LiS^{t}Bu to Cp*MoCl$_4$ in THF formed a dark-red homogeneous solution, from which Cp*Mo(S^{t}Bu)$_3$ (**4**) was isolated as red crystals in 85% yield. Likewise, (PPh$_4$)[Cp*Mo(edt)$_2$] (**5**) was synthesized in 88% isolated yield from the reaction between Cp*MoCl$_4$ and 2.5 equiv of Li$_2$edt in THF followed by cation exchange with PPh$_4$Br in CH$_3$CN. In these reactions, the molybdenum atom was reduced from Mo(V) to Mo(IV), where the reduction was presumably induced by lithium thiolates, and 1 equiv of LiS^{t}Bu and 0.5 equiv of Li$_2$edt were consumed as reducing agents. Indeed, when the stoichiomeric amount of lithium thiolate was used, *i.e.*, 3 equiv for LiS^{t}Bu and 2 equiv for Li$_2$edt, the yields of **4** and **5** were significantly lowered. In the case of the synthesis of **4**, a side product was ^{t}BuSS^{t}Bu according to GC−MS analysis.

The room temperature ^{1}H NMR spectrum of **4** in C_6D_6 shows two sharp singlets at 1.82 and 1.75 ppm in the intensity ratio of 9:5, which were assigned to the protons of *tert*-butyl and Cp* groups, respectively. On the other hand, in the spectrum of **5** in $CDCl_3$, the Cp* and edt signals appear as broad peaks at 2.0 and 2.8 ppm. The expected two multiplets associated with an A_2B_2 pattern for the edt protons in the half-sandwich structure could not be resolved.[19] These NMR data imply that **4** is diamagnetic and conversely **5** assumes a weak paramagnetic nature at room temperature. The observation is consistent with the common magnetic properties of d^2 half-sandwich complexes noted by Poli, in that d^2 $CpMoL_3$ complexes prefer diamagnetic low-spin states, while d^2 $CpMoL_4$ complexes opt for paramagnetism.[20] The difference in magnetism is dictated by the relative energy positioning of the low-lying d orbitals, namely d_{z^2}, d_{xy}, and $d_{x^2-y^2}$.

Although C−S bond cleavage did not take place in the reactions of Cp*MoCl$_4$ with LiS^{t}Bu and Li$_2$edt, the EI-mass spectrum of Cp*Mo(S^{t}Bu)$_3$ (**4**) showed an isotopic cluster corresponding to $[Cp^*MoS_3]^+$. The parent molecular ion peak did not appear in the spectrum, indicating that the C−S bonds of **4** are readily broken in the mass spectrometer. This mass spectrometry derived sulfide complex cation is not likely to be the desired trithio complex, but may be formulated as $[Cp^*Mo^{VI}S(S_2)]^+$. Nevertheless, the observation of facile C−S bond cleavage of ^{t}BuS was quite encouraging to us.

X-ray crystallographic analysis was performed for **4** and **5**. In the case of **5**, the crystal contains phosphonium cations and [Cp*Mo(edt)$_2$] anions with acetonitrile molecules filling a void. The molecular structure of **4** is shown in Figure 1, and the structure of the anion part of **5** is given in Figure 2. Table 2 lists the selected bond distances and bond angles for **4** and **5**.

(19) Tatsumi, K.; Takeda, J.; Sekiguchi, Y.; Kohsaka, M.; Nakamura, A. *Angew. Chem., Int. Ed. Engl.* **1985**, *24*, 332−333.

(20) (a) Krueger, S. T.; Poli, R.; Rheingold, A. L.; Staley, D. L. *Inorg. Chem.* **1989**, *28*, 4599−4607. (b) Abugideiri, F.; Keogh, D. W.; Poli, R. *J. Chem. Soc., Chem. Commun.* **1994**, 2317−2318.

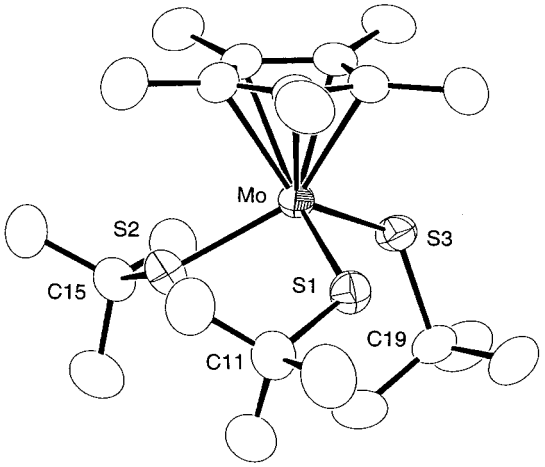

Figure 1. Molecular structure of Cp*Mo(S^{t}Bu)$_3$ (**4**).

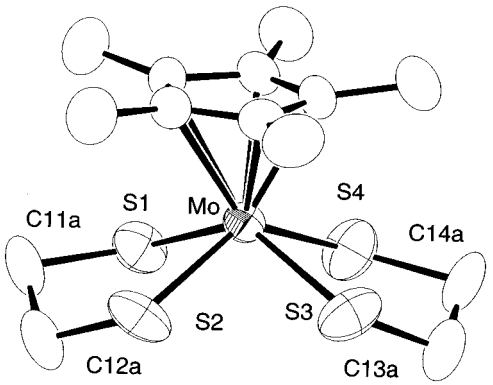

Figure 2. Structure of the anion part of (PPh$_4$)[Cp*Mo(edt)$_2$] (**5**). One set of the disordered carbons of the edt ligands is shown.

Table 2. Selected Bond Distances (Å) and Angles (deg) for Cp*Mo(S^{t}Bu)$_3$ (**4**) and (PPh$_4$)[Cp*Mo(edt)$_2$] (**5**)

	Cp*Mo(S^{t}Bu)$_3$ (**4**)		
Mo−S1	2.3300(7)	S1−Mo−S2	95.13(3)
Mo−S2	2.2956(7)	S1−Mo−S3	97.98(3)
Mo−S3	2.2620(7)	S2−Mo−S3	111.24(3)
S1−C11	1.878(3)	Mo−S1−C11	121.44(10)
S2−C15	1.875(3)	Mo−S2−C15	120.03(9)
S3−C19	1.861(3)	Mo−S3−C19	122.97(9)
		Cp*−Mo−S1−C11	96.2
		Cp*−Mo−S2−C15	98.5
		Cp*−Mo−S3−C19	160.0
	(PPh$_4$)[Cp*Mo(edt)$_2$] (**5**)		
Mo−S1	2.400(1)	S1−Mo−S3	134.43(4)
Mo−S2	2.387(1)	S2−Mo−S4	132.54(5)
Mo−S3	2.396(1)		
Mo−S4	2.368(1)	Mo−S−C(av.)	108.0
S−C(av.)	1.86		

Molecule **4** adopts a pseudotetrahedral arrangement at Mo with one Cp* ring and three sulfurs. The Cp*(centroid)−Mo−S−C torsional angles vary from 96.2° and 98.5° to 160°. Therefore the S−C vectors of ^{t}BuS groups orient in such a way that S1−C11 and S2−C15 nearly parallel the Cp* plane while S3−C19 is perpendicular to it. In the low-spin d^2 configuration, the Mo d_{z^2} orbital is filled with two electrons, leaving low-lying d_{xy} and $d_{x^2-y^2}$ orbitals unoccupied. These vacant d orbitals can in principle participate in π bonding with the occupied S p_π orbitals. However, only the perpendicular orientation of the thiolate is suited for these $d_\pi-p_\pi$ interactions as depicted in Figure 3. This produces the notably shorter Mo−S3 bond (2.2620(7) Å) relative to the Mo−S1 and Mo−S2 distances of 2.3300(7) and 2.2956(7) Å. The mean Mo−S bond length of

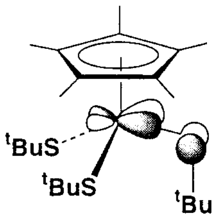

Figure 3. The π bonding between the metal vacant d_π orbital and the occupied S p_π orbital.

2.296 Å is somewhat longer than those found in $Mo(S^tBu)_4$ (2.235(3) Å)[21] and $Mo[S\text{-}2,4,6\text{-}C_6H_2(CHMe_2)_3]_4$ (2.262(1) Å).[22] This elongation may be due to the steric bulk and/or electron-donating properties of the Cp* ligand.

Compound **5** possesses a square-based pyramidal coordination geometry, where Cp* occupies the apical position and the four thiolate sulfur atoms make up the square base. In each MoSCCS five-membered ring, the carbon atoms are disordered, so that two conformations of the ring are superimposed in the structure with an occupancy factor of 50/50. In Figure 2, only one set of these disordered carbons is shown. The mean Mo−S distance is 2.388 Å, which is longer than that of **4** but is slightly shorter than those of the structurally related Mo(IV) thiolate complexes, $(PPh_4)[(C_5H_5)Mo\{S_2C_2(CN)_2\}_2]$ (2.407 Å)[23] and $[N(PPh_3)_2][(C_5H_5)Mo(SC_6F_5)_4]$ (2.420 Å).[24] The two *trans*-S−Mo−S angles in the structure of **5** do not differ much, so that the angular *trans* influence is small for this d^2 bis-dithiolate complex.[25]

Reactions of Cp^*WCl_4 with LiS^tBu and $Li_2(SCH_2CH_2S)$. The reactions of Cp^*MoCl_4 with LiS^tBu and $Li_2(SCH_2CH_2S)$ led uneventfully to the corresponding thiolate complexes **4** and **5** with the concomitant reduction of the molybdenum center to Mo(IV). However, the products obtained from the reactions of the tungsten analogue turned out to be very different.

As Cp^*WCl_4 was treated with 4 equiv of LiS^tBu in THF for 1 h, a homogeneous red solution resulted. Removal of the solvent followed by extraction of the residue with hexane gave a red supernant and a brown solid. The dinuclear sulfide complex **2** was obtained in 20% yield by extraction of the brown solid with toluene, while a standard workup of the hexane extract gave red crystals. The ^1H NMR spectrum of the red compound indicated the presence of one Cp* ligand and one ^tBu group, and the IR spectrum featured two absorptions at 488 and 479 cm^{-1} assignable to the W═S stretching vibrations. Based on these spectroscopic data, coupled with the elemental analysis, this red compound was formulated as $Cp^*W(S)_2(S^tBu)$ (**6**), which was confirmed by X-ray analysis. Thus some of the C−S bonds were cleaved during the reaction giving rise to the disulfido complex **6**, which was isolated in 38% yield. The relatively low yield of **6** is caused partly by thermal instability of the compound in solution. When a THF solution of **6** was kept standing at room temperature, the mononuclear complex turned gradually into the dinuclear sulfide complex **2**, and the metal center was reduced from W(VI) to W(V). Alternatively when the reaction of Cp^*WCl_4 with LiS^tBu was carried out in THF for 12 h, the yield of **2** increased to 58% while only a trace amount of **6** remained.

(21) Otsuka, S.; Kamata, M.; Hirotsu, K.; Higuchi, T. *J. Am. Chem. Soc.* **1981**, *103*, 3011−3014.

(22) Roland, E.; Walborsky, E. C.; Dewan, J. C.; Schrock, R. R. *J. Am. Chem. Soc.* **1985**, *107*, 5795−5797.

(23) Churchill, M. R.; Cooke, J. *J. Chem. Soc. A* **1970**, 2046−2053.

(24) Wan Abu Bakar, W. A.; Davidson, J. L.; Lindsell, W. E.; McCullough, K. J. *J. Chem. Soc., Dalton Trans.* **1990**, 61−71.

(25) (a) Poli, R. *Organometallics* **1990**, *9*, 1892−1900. (b) Lin, Z.; Hall, M. B. *Organometallics* **1993**, *12*, 19−23.

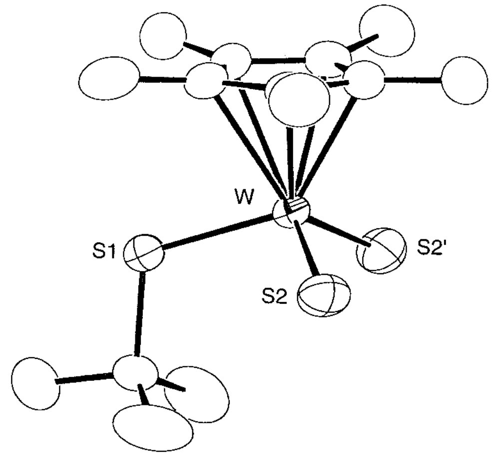

Figure 4. Molecular structure of $Cp^*W(S)_2(S^tBu)$ (**6**).

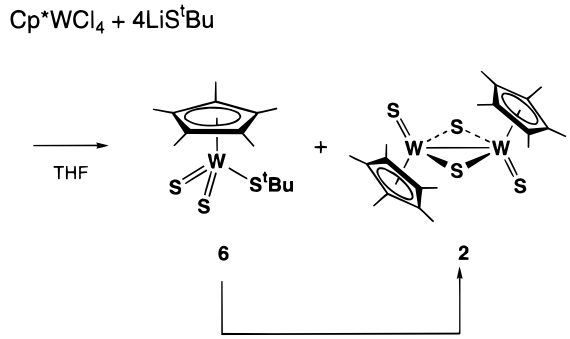

(4)

The X-ray derived structure of **6** is shown in Figure 4, and the selected metric parameters are given in Table 3. The crystal belongs to the centrosymmetric space group of *Pnma*, and a crystallographic mirror plane passes through the molecule, where W, S1, C1, C3, and C6 sit on the plane. The *tert*-butyl group points away from the Cp* ring presumably to avoid steric congestion, and the S−C vector is oriented perpendicular to the ring. In the W(VI) oxidation state, all three low−lying d orbitals are unoccupied, so that both the thiolate and thio ligands can form $p_\pi-d_\pi$ bonds.

The reaction between Cp^*WCl_4 and 2 equiv of Li_2edt in THF gave an orange-red homogeneous solution. Inspection of the solution by UV−visible spectroscopy showed a strong absorption band at 377 nm which is characteristic of $[Cp^*W(S)_3]^-$. This unexpected observation was corroborated by the successful isolation of $(PPh_4)[Cp^*W(S)_3]$ (**3**) which was obtained by standard workup of the THF solution and subsequent cation exchange with PPh_4Br in CH_3CN.

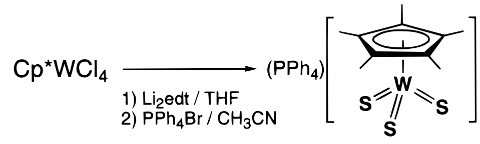

3, 82%

(5)

By analogy to the molybdenum system, it seems likely that the above reaction first forms the bis-dithiolate complex $[Cp^*W(edt)_2]^-$ and C−S bond rupture follows. This is not an unthinkable assumption, because we were able to isolate a closely related propanedithiolato complex $(PPh_4)[Cp^*W(pdt)_2]$ (pdt = $SCH_2CH_2CH_2S$) from a similar reaction with Li_2pdt.[26]

(26) Kawaguchi, H.; Tatsumi, K. To be published.

Table 3. Selected Bond Distances (Å) and Angles (deg) for $Cp^*W(S)_2(S^tBu)$ (**6**) and $Cp^*Mo(E)_2(S^tBu)$ (E = O (**7**), S (**8**))

	M = W, E = S (**6**)	M = Mo, E = O (**7**)	M = Mo, E = S (**8**)
M═E	2.147(2)	1.713(3)	2.136(1)
M−S1	2.345(2)	2.363(1)	2.354(1)
S1−C1	1.850(9)	1.864(1)	1.874(5)
E−M−E′	105.6(1)	107.2(2)	105.88(7)
E−M−S1	105.4(1)	105.14(9)	105.65(4)
M−S1−C1	113.5(3)	107.9(2)	112.9(2)

The difference in stability between $[Cp^*Mo(edt)_2]^-$ and the putative intermediate $[Cp^*W(edt)_2]^-$ could arise from the redox properties of the metal atoms. Tungsten is known to be oxidized more readily than molybdenum, if the reaction condition allows it. Although a detailed mechanistic study is still needed, we hypothesize that C−S bond activation would be promoted when thiolate complexes are prone to be oxidized. This argument applies also to the aforementioned reaction of Cp^*WCl_4 with LiS^tBu to give $Cp^*W(S)_2(S^tBu)$ (**6**). Regardless of the detailed mechanism of the C−S bond cleavage step, our finding demonstrates that metal-mediated C−S bond cleavage reactions offer a novel synthetic route to thio complexes.[18]

Attempts To Synthesize the Trithio Complex of Molybdenum $[Cp^*Mo(S)_3]^-$. The successful synthesis of mononuclear thio complexes of tungsten via C−S bond cleavage reactions prompted us to examine the conversion of the molybdenum thiolate analogues into the relevant thio complexes. The half-sandwich molybdenum thiolate complexes are thermally robust. For instance, the ethanedithiolate complex $(PPh_4)[Cp^*Mo(edt)_2]$ (**5**) shows no sign of C−S bond rupture at 50−60 °C in THF/CH_3CN, but it was found to decompose gradually in boiling DMF under argon. Under this rigorous thermodecomposition condition, however, liberation of Cp* or dinuclearization took place to give $(PPh_4)_2[Mo(S)_4]$ and $Cp^*_2Mo_2(S)_2(\mu\text{-}S)_2$ (**1**) in 26% and 23% yields, and the desired mononuclear thio complexes were not obtained. To this end we planned to chemically oxidize the thiolate complexes under mild conditions, hoping that C−S bond activation may be promoted in a controlled manner. We thus investigated reactions of **5** and $Cp^*Mo(S^tBu)_3$ (**4**) with oxidants such as O_2, hydrazines, elemental sulfur, and elemental selenium. We found that such reactions of the latter thiolate complex **4** are promising, and the results are described in the following chapters.

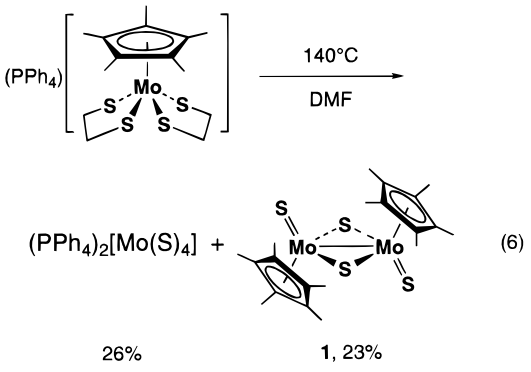

(A) Reaction of 4 with O_2. The complex **4** was found to react readily with 1 atmosphere of dry O_2. According to an NMR tube experiment in C_6D_6, the reaction proceeds cleanly and produces $Cp^*Mo(O)_2(S^tBu)$ (**7**) and $^tBuSS^tBu$, quantitatively. On a preparative scale, **7** was obtained as yellow crystals in 83% yield after recrystallization from hexane. The reductive elimination of *tert*-butyl thiolate and the concomitant oxidative addition of O_2 induces a net oxidation of molybdenum from Mo(IV) to Mo(VI). Interestingly, one of the three ^{t}BuS ligands of **4** remains intact during this reaction. Although the oxidation of **4** by O_2 did not produce the target thio complex, this reaction turns out to be a convenient entry into an intriguing dioxo−thiolate complex. The IR spectrum of **7** shows two Mo═O stretching bands at 901 and 875 cm^{-1}, which are comparable to those of $Cp^*Mo(O)_2[OSi(CH_2Ph)_3]$ (923 and 871 cm^{-1}).[27] According to the X-ray analysis, the crystal of **7** is isomorphous to that of **6** and their structures are very much alike, where a mirror plane runs through the molecule. Selected bond distances and angles are given in the second column of Table 3. The Mo═O bond length is normal.[28]

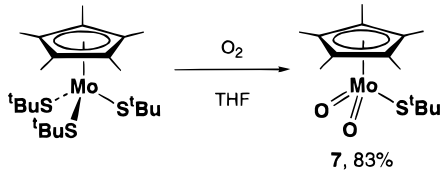

(B) Reactions of 4 with Hydrazines. Complex **4** reacted slowly with NH_2NMe_2 in THF at room temperature over several days to give a brown solution, from which the mononuclear thio complex $Cp^*Mo(S)_2(S^tBu)$ (**8**) was obtained as brown crystals. The bis-thio structure was inferred from the spectroscopic data and elemental analysis, and was established by X-ray. The use of NH_2NHPh also gave rise to **8**, and again the reaction proceeded slowly. The EI-mass spectrum of **8** is featured by an isotopic cluster of peaks corresponding to the $[Cp^*MoS_3]^+$ fragment, while the signals of the parent molecular ion are absent. The situation is very similar to the mass spectrum of $Cp^*Mo(S^tBu)_3$ (**4**).

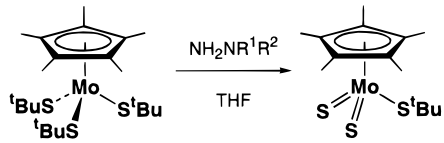

The yield of **8** was relatively poor in either of the reactions. Nevertheless the discovery of C−S bond activation by hydrazines to give the rare *cis*-$Mo(S)_2$ moiety expanded the scope of our effort. The C−S bond cleavage reactions of *tert*-butylthiolate may follow one of the three possible pathways: (a) an internal redox reaction which reduces the C−S bond while oxidizing the metal ion, (b) a heterolytic route generating isobutene via a *tert*-butylcarbonium ion intermediate, or (c) a homolytic route generating isobutane via hydrogen abstraction by a *tert*-butyl radical intermediate. Route b is thought to be favored when a base assists deprotonation of a nascent *tert*-butylcarbonium ion. However this pathway appears to be ruled out for the reaction of **4** because isobutene was not detected in the products and because **4** did not react with LiS^tBu nor NEt_3. Therefore it is unlikely that hydrazines acted as bases in the C−S bond cleaving reactions of **4**. The GC−MS and ^{1}H NMR

(27) Rau, M. S.; Kretz, C. M.; Geoffroy, G. L.; Rheingold, A. L.; Haggerty, B. S. *Organometallics* **1994**, *13*, 1624−1634.
(28) Nugent, W. A.; Mayer, J. M. *Metal−Ligand Multiple Bonds*; John Wiley and Sons: New York, 1988.

analyses revealed formation of isobutane, and aniline was also detected for the reaction with NH_2NHPh. Although the role of hydrazines is still unclear, the N−N bond rupture might have caused oxidation of the metal which in turn induced C−S bond activation.

The crystal of **8** is isomorphous to those of **6** and **7**, and selected bond distances and angles are given in the third column of Table 3. Comparison of the structures of the three closely related complexes in Table 3 is of interest. The M−S^{t}Bu bond distance elongates in the order **6** < **8** < **7**, which parallels the decrease of the M−S−C angle. The combination of these geometric parameters can be a measure of M d_π−Sp$_\pi$ interactions, *i.e.*, weakening of the M−S π bonding leads to a longer M−S distance and a smaller M−S−C angle.[18c,29] Thus the observed trend indicates that the M−S^{t}Bu π bonding interaction decreases in going from **6** to **8** and to **7**. We interpret the result as a consequence of the reverse order of the M═E π bond strength, leading to the conclusion that the amount of π electron donation from E increases in the order W═S < Mo═S < Mo═O.

(C) Reaction of 4 with Elemental Sulfur. The reaction between **4** and $^1/_4$ equiv of S_8 in THF at room temperature proceeded with a gradual color change from dark red to dark green, from which we obtained four compounds. Extraction of the reaction mixture with hexane left a brown residue, and *anti*-Cp*$_2$Mo$_2$(S)$_2$(μ-S)$_2$ (**1**) (12%) was obtained therefrom. On the other hand, red and green crystals grew from the hexane extract and they were separated manually. The ^{1}H NMR spectrum of the red crystals consists of two sets of Cp* and ^{t}Bu proton signals, one of which was assignable to Cp*Mo(S)$_2$(S^{t}Bu) (**8**). In the IR spectrum, there appeared a band at 890 cm^{-1} arising from a Mo═O stretching vibration, in addition to the Mo═S band at 485 cm^{-1}. Furthermore, the mass spectrum revealed two isotopic clusters corresponding to Cp*MoS$_3^+$ and Cp*MoS$_2$O$^+$. Thus the seemingly pure crystalline red material **8** contains an additional compound that carries the Mo═O moiety. Inspection of the above spectroscopic data indicated that the second compound is not Cp*Mo(O)$_2$(^{t}Bu) (**7**), but Cp*Mo(O)(S)(^{t}Bu) (**9**). X-ray analysis of a red single crystal gave a cell dimension of a = 8.514(2) Å, b = 12.041(3) Å, c = 16.421(4) Å, and V = 1683.5(7) Å^3 with the *Pnma* space group, the cell size of which falls in between those of isomorphic crystals of **7** and **8**. The careful structure refinements suggested that the crystal was in fact compositionally disordered between **8** and **9**.

The ratio of **8** and **9** in the red crystals varies from 1:1 to 3:1, depending on the reaction batch, as monitored by ^{1}H NMR spectroscopy, and the yield of **8** is in the range 12%−35%. Although the above synthesis was pursued by a conventional Schlenk technique using dry solvents, the oxo ligand of **9** is most likely to originate from adventitious H_2O. Even if we carried out the reaction in a glovebox under an N_2 atmosphere where contamination by O_2 and H_2O was maintained to be less than 1 ppm, the yield of **9** was found to decrease only slightly.

Characterization of the green crystals by ^{1}H NMR has been hampered by its paramagnetic nature. The IR spectrum indicates the presence of Cp*, but Mo═O and Mo═S bands were absent. Interestingly, upon standing for a long period, a THF solution of the green compound was partially converted into a mixture of **1**, **8**, and **9**. The growth of single crystals of this green compound suitable for an X-ray diffraction study has been unsuccessful so far.

(29) Albright, T. A.; Burdett, J. K.; Whangbo, M. H. *Orbital Interactions in Chemistry*; John Wiley and Sons: New York, 1985

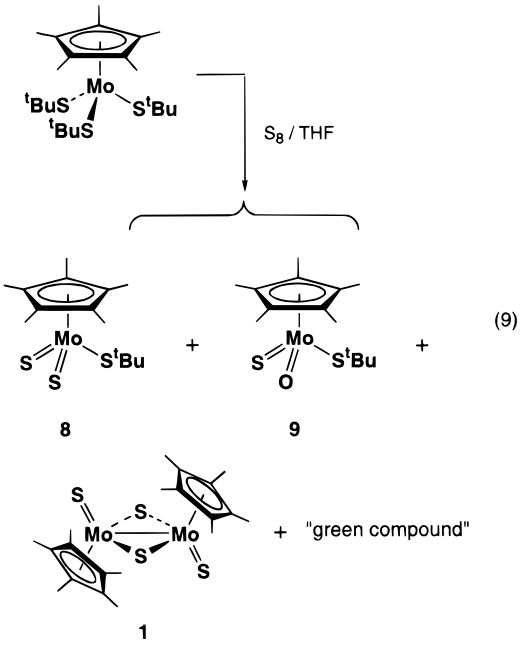

(9)

8 **9** **1**

(D) Reaction of 4 with Selenium. We then treated **4** with 2 equiv of grey selenium in THF at room temperature. An appropriate workup and recrystallization of the reaction mixture resulted in red and purple crystalline materials. The red compound was identified as Cp*Mo(S)$_2$(S^{t}Bu) (**8**) (33% yield) on the basis of spectroscopic data. The ^{1}H NMR spectrum of the purple compound showed two Cp* singlets with the intensity ratio of 2:1, and the IR spectrum gave a Mo═S band at 485 cm^{-1}. The X-ray analysis revealed a dinuclear structure *anti*-Cp*$_2$Mo$_2$(E)$_2$(μ-E)$_2$ (**10**) in which a crystallographic inversion center resides at the center of the molecule. Both the terminal and bridging positions (E) were found to be compositionally disordered between S and Se. Constraining both the positional and thermal parameters of S and Se to be the same at each position, we refined the occupancy factors to be Se(70%)/S(30%) for the terminal chalcogen and Se(46%)/S(54%) for the bridging chalcogen.

An interesting aspect of the reactions of **4** with sulfur and selenium is that both reactions produced the common dithio complex **8** in moderate yields. The absence of Cp*Mo(S)(Se)(S^{t}Bu) and Cp*Mo(Se)$_2$(S^{t}Bu) in the products of the latter reaction suggests that C−S bond cleavage of S^{t}Bu occurred in a specific manner, and that the thio ligand of **8** derived from the **4**/S_8 reaction system also originated from a *tert*-butyl thiolate of **4**.

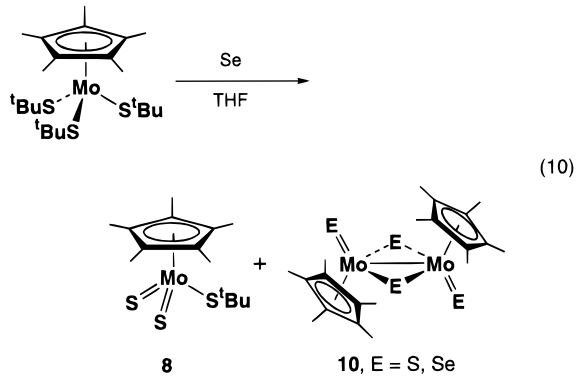

(10)

8 **10**, E = S, Se

(E) Finally to (PPh$_4$)[Cp*Mo(S)$_3$] (11). The successful synthesis of the mononuclear Mo(VI) dithio complex **8** led us to envision replacement of the remaining *tert*-butyl thiolate

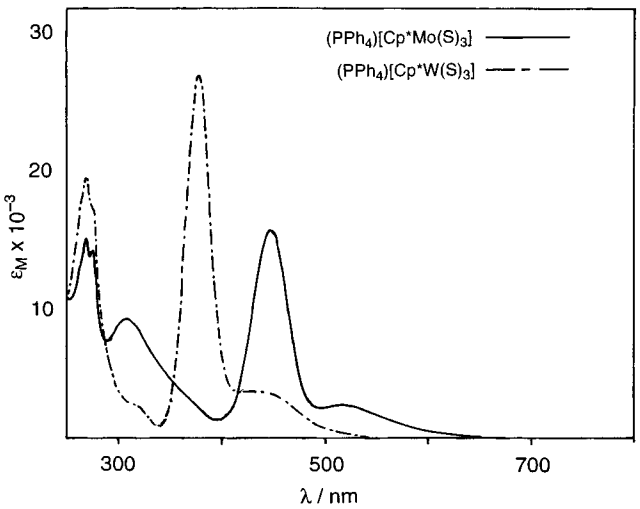

Figure 5. UV−visible spectra of $(PPh_4)[Cp^*M(S)_3]$ (M = W (**3**), Mo (**11**)) in CH_3CN.

group by S^{2-}. In the light of our previous finding that the sulfide reagent, Li_2S_2, reacted with $Cp^*Ta(SCH_2CH_2S)_2$ and $Cp^*TaCl(S)(SCPh_3)$, resulting in formation of $[Cp^*Ta(S)_3Li_2(THF)_2]_2$,[11b,30] we employed a similar strategy for the transformation of **8** to the trithio complex.

When the reaction between **8** and Li_2S_2 in THF was monitored by UV−visible spectroscopy, absorption bands at 450 and 520 nm (sh) emerged and their intensity increased gradually with decrease of the bands associated with **8**. The newly emerged spectroscopic pattern resembles the spectrum of $(PPh_4)[Cp^*W(S)_3]$ (**3**) in CH_3CN, which has the absorption maxima at 377 and 428 nm (sh) as shown in Figure 5. Indeed cation exchange of the reaction product with PPh_4Br in CH_3CN and subsequent purification gave rise to the target complex $(PPh_4)[Cp^*Mo(S)_3]$ (**11**) as red crystals in 65% yield. Noteworthy here is the thermodynamic stability of the molybdenum trithio complex. Once the Mo(VI)═S bonds are formed, the complex does not show a tendency to degrade through self-reduction.

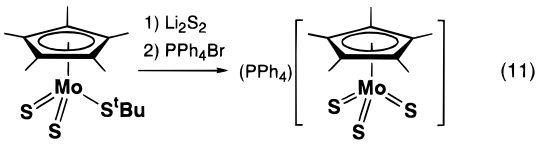

(11)

11,65%

The red (bathochromic) shift of the absorption bands in going from **3** to **11** (446 and 516 nm in CH_3CN) amounts to ca. 0.5 eV. The size of the red shift is somewhat larger than that for $Cp^*W(S)_2(S^tBu)$ (**6**) and $Cp^*Mo(S)_2(S^tBu)$ (**8**), but their systematic shifts to higher wavelengths prove that the absorptions must arise from sulfur-to-metal charge-transfer transitions, and imply lower positioning of the vacant Mo 4d energy level relative to the W 5d orbitals. Incidentally the bathochromic shift of 0.5 eV is close to the value observed for the UV−visible spectra of $(PPh_4)[M(SCH_2CH_2S)_3]$ and $(PPh_4)[M(SCH_2CH_2CH_2S)_3]$ (M = Ta, Nb).[31]

In the IR spectrum, the Mo═S bands appear at 445 and 455 cm^{-1}, which can be assigned to the E and A_1 normal stretching modes for the pyramidalized C_{3v} MoS_3 unit. The corresponding bands for the tungsten analogue, **6**, were observed at 437 and 466 cm^{-1}. The Mo═S stretching bands for **11** are clearly shifted to lower energies relative to the corresponding IR bands for **8** (485 cm^{-1}) and $[Mo(S)_4]^{2-}$ (458 and 472 cm^{-1}).[32] The trend is in harmony with the Mo═S bond lengths determined by the X-ray analysis. Figure 6 presents the three-legged piano stool structure of the anion of **11**, and Table 4 compares the selected bond distances and angles with those of **3**. Both the Mo═S distances and S═Mo═S angles of **11** are practically the same as the analogous geometric parameters of **3**. This observation is not surprising considering the nearly identical ionic radii of six-coordinate Mo(VI) and W(VI).[33] The mean Mo═S distance of 2.188 Å is longer by 0.052 Å than that of **8**. The weakening of the Mo═S bond on going from the dithio complex to the trithio complex is understandable because the σ and π donation of electrons from S to Mo per each Mo═S bond would decrease as the number of strong S^{2-} donor ligands at the same metal center increases. In this regard, it is intriguing that the Mo═S bond of **11** is even longer than that of $(NH_4)_2[Mo(S)_4]$ (2.178 Å).[34] The steric bulk and electron-donor character of Cp* may contribute to this unusual trend. The small S═Mo═S angle of 105.2°, less than the tetrahedral value, is consistent with the above argument. Similarly, the mean W═S bond length (2.192 Å) of $(PPh_4)[Cp^*W(S)_3]$ (**3**) is long compared with that of $(NH_4)_2[W(S)_4]$ (2.177 Å).[4]

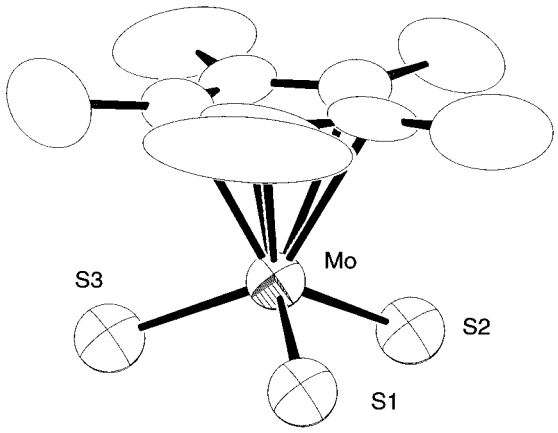

Figure 6. Structure of the anion part of $(PPh_4)[Cp^*Mo(S)_3]$ (**11**).

Table 4. Selected Bond Distances (Å) and Angles (deg) for $(PPh_4)[Cp^*M(S)_3]$ (E = W (**3**), Mo (**11**))

	M = W (**3**)	M = Mo (**11**)
M−S1	2.189(2)	2.187(3)
M−S2	2.199(2)	2.195(3)
M−S3	2.188(2)	2.183(3)
S1−M−S2	105.31(9)	105.8(1)
S1−M−S3	104.23(9)	104.7(1)
S2−M−S3	104.93(9)	105.2(1)

The isolated yield of **11** in the reaction between **8** and Li_2S_2 is acceptable. However the reaction of **4** with hydrazine to give the precursor **8** proceeds very slowly, and the yield is relatively low. Isolation of **8** in pure form from the **4**/S_8 (or Se) reaction system is also a tedious task, and the yield is again low. Therefore we were driven to find a better method to synthesize **11**. Since the problem arose in isolating the precursor, we attempted a one-pot reaction of **4**, 1/4 equiv of S_8, and Li_2S_2 in THF, which is referred to as Method A in the Experimental

(30) Kawaguchi, H.; Tatsumi, K. *Organometallics* **1997**, *16*, 307−309.
(31) Tatsumi, K.; Matsubara, I; Sekiguchi, Y.; Nakamura, A.; Meali, C. *Inorg. Chem.* **1989**, *28*, 773−780.
(32) (a) Schmidt, K. H.; Müller, A. *Spectrochim. Acta* **1972**, *28A*, 1829−1840. (b) Müller, A.; Weinstock, N.; Schulze, H. *Spectrochim. Acta* **1972**, *28A*, 1075−1082.
(33) Schannon, R. D. *Acta Crystallogr. Sec A* **1976**, *32*, 751−767.
(34) Lapasset, J.; Chezeau, N.; Belougne, P. *Acta Crystallogr. Sec B* **1976**, *32*, 3087−3088.

Scheme 1

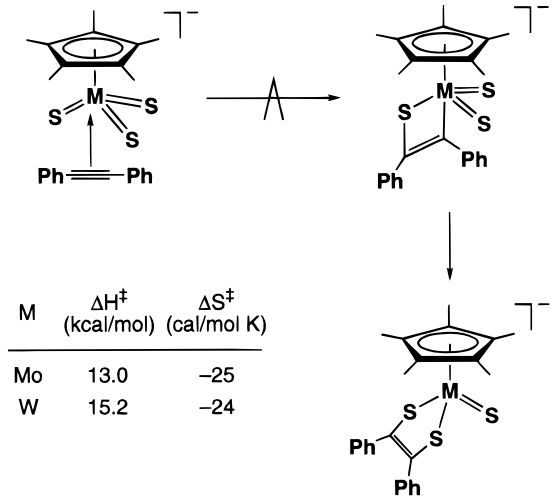

Section. Thus after treating **4** and $^1/_4$ S_8 in THF for 12 h at room temperature, the resulting green solution was directly added to Li_2S_2 and the reaction mixture was stirred for another 12 h. The green color of the solution turned gradually to red, and the THF solvent was replaced by CH_3CN for the subsequent cation exchange reaction with PPh_4Br. From the above procedure, **11** was isolated in 56% yield. Although the dinuclear complex **1** was also formed as a side product, it could be separated easily from **11** by virtue of their different solubilities in THF. Upon isolation of **8** from the reaction mixture of **4**/S_8, we suffered from contamination of the product by Cp*Mo(O)(S)(^{t}-Bu) (**9**). In contrast, the one-pot synthesis of **11** did not give oxo species such as $[Cp^*Mo(O)(S)_2]^-$ according to the IR and mass spectrometry analyses.

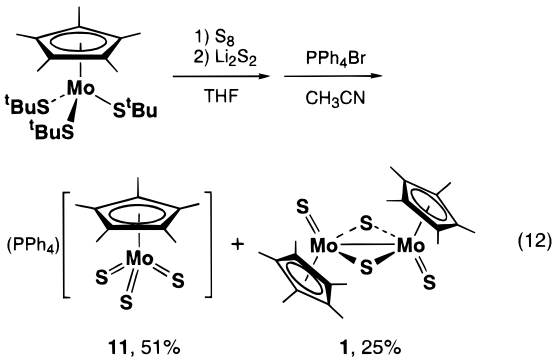

Reactions of $(PPh_4)[Cp^*M(S)_3]$ (M = Mo, W) with Diphenylacetylene. Tetrathiometalates such as $[Mo(S)_4]^{2-}$, $[W(S)_4]^{2-}$, $[V(S)_4]^{3-}$, and $[Re(S)_4]^-$ are known to serve as synthetic precursors of a broad spectrum of heterometallic sulfide clusters.[4,35] Likewise, the half-sandwich trithio complex of tantalum $[Cp^*Ta(S)_3Li_2(THF)_2]_2$ was found to react readily with halo complexes of late-transition metals to form TaM_2 trinuclear clusters.[12,36] On the other hand, reactions of organic substrates at terminal sulfido ligands are less frequently observed. We have recently communicated that $(PPh_4)[Cp^*W(S)_3]$ (**3**) reacted with PhC≡CPh and PhC≡CH to afford the corresponding 1,2-enedithiolato complexes, $(PPh_4)[Cp^*W(S)(S_2C_2PhR)]$ (R = Ph, H). Here we present a detailed account of the addition reactions of diphenylacetylene to the terminal thio groups in $(PPh_4)[Cp^*W(S)_3]$ (**3**) and $(PPh_4)[Cp^*Mo(S)_3]$ (**11**).

Upon treating **3** with excess diphenylacetylene at room temperature in CH_3CN, we noticed a gradual color change of the solution from orange to green, and $(PPh_4)[Cp^*W(S)(S_2C_2Ph_2)]$ (**12**) was isolated therefrom as yellow-green crystals. According to an NMR experiment, this reaction proceeds very cleanly and **3** is transformed quantitatively to **12**. The analogous reaction of $(PPh_4)[Cp^*Mo(S)_3]$ (**11**) with PhC≡CPh again took place smoothly affording $(PPh_4)[Cp^*Mo(S)(S_2C_2Ph_2)]$ (**13**) as brown plates.

Table 5. Selected Bond Distances (Å) and Angles (deg) for $(PPh_4)[Cp^*M(S)(S_2C_2Ph_2)]$ (E = W (**12**), Mo (**13**))

	M = W (**12**)	M = Mo (**13**)
M−S1	2.186(2)	2.177(2)
M−S2	2.318(2)	2.307(2)
M−S3	2.334(2)	2.335(2)
S2−C11	1.782(6)	1.773(6)
S3−C12	1.799(6)	1.791(6)
C11−C12	1.35(1)	1.329(8)
S1−M−S2	108.3(1)	108.25(8)
S1−M−S3	109.6(1)	110.29(9)
S2−M−S3	82.5(1)	82.01(6)
M−S2−C11	110.5(2)	110.3(2)
M−S3−C12	109.7(2)	110.0(2)

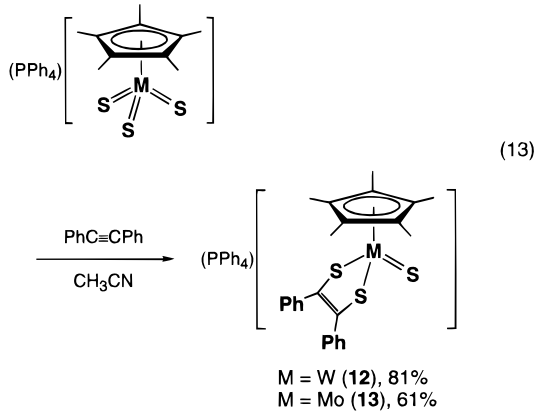

It should be mentioned here that neither $[W(S)_4]^{2-}$ nor $[Mo(S)_4]^{2-}$ is reactive toward PhC≡CPh. The higher reactivity of the terminal thio groups of **3** and **11** may be related to the notably long M═S distances compared with those of the tetrathiometalates. As was discussed earlier in this paper, the longer M═S bonds are ascribable to the steric bulk and/or strong electron-donating character of the Cp* ligand, which in turn results in decrease of π electron donation from S to M. These effects, however, do not explain the enhanced reactivity of the thio ligands of **3** and **11** toward nucleophilic alkynes. Direct addition of PhC≡CPh to the negatively charged thio groups appear to be a difficult pathway, and we prefer the stepwise mechanism shown in Scheme 1, where the alkyne interacts first with the electron-deficient metal center, forms an four-centered metallathiabutene intermediate (or transition state), and then subsequently rearranges leads to from the 1,2-enedithiolate structure.

The X-ray crystal structure of **13** is practically identical to the tungsten congener **12**,[10] and Table 5 compares their selected bond distances and angles. The M═S distances of **12** and **13** are distinctively longer than those of $Cp^*W(S)_2(SCH_2Ph)$ (2.149(2) Å) and $Cp^*Mo(S)_2(S^tBu)$ (**8**) (2.136(1) Å), respectively, and the lengthening is consistent with their lower M═S stretching frequencies of 465 cm^{-1} (**12**) and 469 cm^{-1} (**13**).

(35) (a) Holm, R. H. *Adv. Inorg. Chem.* **1992**, *38*, 1−71. (b) Coucouvanis, D. *Acc. Chem. Res.* **1981**, *14*, 201 −209.

(36) (a) Lang, J.; Kawaguchi, H.; Ohnishi, S.; Tatsumi, K. *J. Chem. Soc., Chem. Commun.* **1997**, 405−406. (b) Lang. J.; Kawaguchi, H.; Yamada, K.; Tatsumi, K. To be published.

Chart 2

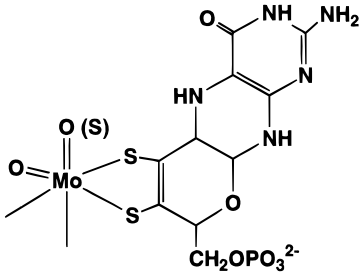

Coordination of 1,2-enedithiolato occurs with a planar MS_2C_2 ring conformation, suggesting π-electron delocalization over all five atoms. In fact the averaged S−C distance of 1.786 Å is significantly shorter than the S−C single bond lengths in **4**, **5**, **7**, and **8**. However, the C−C distances are as short as 1.35(1) Å (**12**) and 1.329(8) Å (**13**) implying, contrary to the above argument, localization of π-bonding in the C−C bond. There is dichotomy between 1,2-enedithiolato(2−) and 1,2-dithiolene-(0) structures in describing the coordination mode of SCRCRS. According to the observed geometric parameters, reality may well be between the two extremes, perhaps leaning rather toward the 1,2-enedithiolato(2−) structure.

To gain some insight into the kinetics of formation of **12** and **13**, we monitored the disappearance of Cp* resonances in the ^{1}H NMR spectra of the reactants, **3** and **11**, in DMF-d_7 under pseudo-first-order conditions with excess PhC≡CPh. We confirmed that appearance of the Cp* signal of either product is exactly complementary to disappearance of the reactant Cp* signal. The phenyl proton signals of the 1,2-enedithiolate of **12** or **13**, which appear separately from the phenyl signals of $(PPh_4)^+$, also increased in parallel with the increase of the Cp* signal. All plots of ln[**3**] or ln[**11**] against time were linear up to complete conversion to **12** or **13**, where correlation coefficients were greater than 0.993. The observed pseudo-first-order rate constants k_{obs} were found to linearly correlate with PhC≡CPh concentration, pointing to a first-order dependence of the reactions on PhC≡CPh concentration. Dividing k_{obs} by the concentration of PhC≡CPh yielded the second-order rate constant k_2 (see Experimental Section), first order in both PhC≡CPh and $(PPh_4)[Cp^*M(S)_3]$. Eyring plots generated straight lines with correlation coefficients being 1.00 and 0.993 (see Supporting Information), from which activation parameters were determined. These are $\Delta H^‡ = 15.2$ kcal/mol and $\Delta S^‡ = -24$ cal/mol K for the reaction of **3**, and $\Delta H^‡ = 13.0$ kcal/mol and $\Delta S^‡ = -25$ cal/mol K for the reaction of **11**. The negative entropy of activation accords with a bimolecular rate-determining step, and the nearly identical $\Delta S^‡$ values for **3** and **11** suggest that the two reactions take place by a common mechanism. Evidently the addition reaction of PhC≡CPh to the trithio complex of tungsten is slower than that of molybdenum. The observed trend can be understood on the basis of the ease with which the metal center is reduced from M(VI) to M(IV). Molybdenum is known to favor lower oxidation states in comparison with tungsten.

Recently interest in 1,2-enedithiolato complexes of molybdenum and tungsten arose from a structural study of the Mo-(W)-containing oxotransferase enzymes, a common constitution of which is featured by coordination of pterine-1,2-enedithiolate.[37] Chart 2 illustrates an example of the foreshadowed structures of the enzymes.[38] The usual synthetic route to mononuclear 1,2-enedithiolato complexes of molybdenum is reactions of preformed salts of 1,2-enedithiolates with appropriate molybdenum halides,[39] while the reaction of polythiomolybdenum compounds with activated alkynes such as MeOCOC≡CC(O)OMe (DMCA) and $CF_3C≡CCF_3$ have offered another method.[40] However, the complexes **12** and **13** are unique in that both a thio group and a 1,2-enedithiolate unit coordinate at a single metal center.

The direct addition of an alkyne to a bridging monothio ligand is rare. Examples include the reactions of $(C_5H_5)_2Mo_2(\mu\text{-}S)_2(\mu\text{-}SH)_2$,[41] $(C_5H_4Me)_2V_2(\mu\text{-}S)_2(\mu\text{-}S_2)$,[42] and $[Mo_3(\mu_3{-}S)(\mu\text{-}O)(\mu\text{-}S)_2(H_2O)_9]^{4+}$ [43] with a series of alkynes.[44] The reaction of an alkyne at a terminal thio ligand is more unusual. However one closely related to our reactions is the formation of a 1,2-enedithiolato ligand by addition of DMAC to $\{HB(Me_2pz)_3\}$-$W(S)_2X$ (X = OPh, SPh, SePh).[45] Our results show that thio groups on Mo(VI) and W(VI) are capable of reacting even with nonactivated alkynes. Recently, $[Re(S)_4]^-$ was found to react readily with alkynes and alkenes, and further addition of S_8 or amine oxide generated $Re(E)(SCR{=}CRS)_2$ (E = O, S) and $Re(S)(S_4)(SCH_2CH_2S)$.[46] Interestingly $Cp^*_2Zr(S)L$ (L = pyridine, 4-*tert*-butylpyridine) undergoes a [2+2] cycloaddition with RC≡CR (R = Et, Ph, Tol) to give $Cp^*_2Zr(SCR{=}CR)$.[47]

Another aspect which merits comment is comparison of reaction patterns between M=S and M=O toward alkynes. The trioxo complex $Cp^*Re(O)_3$, which is isoelectronic and isostructural to $[Cp^*M(S)_3]^-$ (M = Mo (**11**), W (**3**)), was reported to react with alkynes when PPh_3 was present, resulting in the formation of the intriguing 1-rhena-4-oxacyclohexa-2,5-diene ring.[48] The kinetics of extrusion of alkenes from $Cp^*Re(O)$-[OCH(R)CH(R)O] and those of the reverse reactions were examined in detail.[49] The resulting energetics implied a stepwise mechanism with a metallaoxetane intermediate which is analogous to that shown in Scheme 1. The activation enthalpies measured for the alkene addition reactions to $Cp^*Re(O)_3$ vary from 11.7 to 18.2 kcal/mol, and the $\Delta H^‡$ values for the reactions of **3** and **11** with diphenylacetylene fall in this range. In the case of another oxo analogue of **3**, $[Cp^*W(O)_3]^-$, the reaction with 2 equiv of DMAC afforded the [2+2+2] cycloaddition product $[(Ph_3P)_2N][Cp^*(O)_2W(OC(R){=}C(R)C(R){=}CR)]$ (R=C-

(37) (a) Ramao, M.; Archer, M.; Moura, J. J. G.; LeGall, J.; Engh, R.; Scheider, M.; Hof, P.; Huber, R. *Science* **1995**, *270*, 1170−1176. (b) Schindelin, H.; Kisker, C.; Hilton, J.; Rajagopalan, K. V.; Reeds, D. C. *Science* **1996**, *272*, 1615−1621, (c) Chan, M. K.; Makund, W.; Kletzin, A.; Adams, M. W. W.; Reeds, D. C. *Science* **1995**, *267*, 1463−1469.

(38) (a) Collison, D.; Garner, C. D.; Joule, J. A. *Chem. Soc. Rev.* **1996**, 25−32. (b) Hsu, J. K.; Bonangelino, C. J.; Kaiwar, S. P.; Boggs, C. M.; Fettinger, J. C.; Pilato, R. S. *Inorg.Chem.* **1996**, *35*, 4743−4751.

(39) (a) Oku, H.; Ueyama, N.; Nakamura, A.; Kai, Y.; Kanehisa, N. *Chem. Lett.* **1994**, 607−610. (b) Tatsumi, K.; Matsubara, I.; Sekiguchi, Y.; Nakamura, A.; Meali, C. *Inorg. Chem.* **1989**, *28*, 773−780. (c) Martin, J. L.; Takats, J. *Inorg. Chem.* **1975**, *14*, 73−78.

(40) (a) Coucouvanis, D.; Toupadakis, A.; Koo, A.-M.; Hadjikyriacou, A. *Polyhedron* **1989**, *8*, 1705−1716. (b) Coucouvanis, D.; Hadjikyricacou, A.; Koo, S.-M.; Ileperuma, O.; Draganjac, M.; Salifoglou, A. *Inorg. Chem.* **1991**, *30*, 754−767.

(41) Rakowski DuBois, M.; VanDerreer, M. C.; DuBois, D. L.; Haltiwanger, R. C.; Miller, W. K. *J. Am. Chem. Soc.* **1980**, *102*, 7456−7461.

(42) Bolinger, C. M.; Rauchfuss, T. B.; Rheingold, A. L. *J. Am. Chem. Soc.* **1983**, *105*, 6321−6323.

(43) Shibahara, T.; Sakane, G.; Mochida, S. *J. Am. Chem. Soc.* **1993**, *115*, 10408−10409.

(44) Addition of acetylene to the disulfido ligands of $[Cp^*_2Re_2(\mu\text{-}S_2)_2]^{2+}$ and $Cp^*_2Ru_2(\mu,\eta^2\text{-}S_2)(\mu,\eta^1\text{-}S_2)$ has been observed. (a) Rakowski DuBois, M.; Jagirdar, B. R.; Diez, S.; Noll, B. C. *Organometallics* **1997**, *16*, 294−296. (b) Rauchfuss, T. B.; Rodgers, D. P. S.; Wilson, S. R. *J. Am. Chem. Soc.* **1986**, *108*, 3114−3115.

(45) Eagle, A. A.; Harben, S. M.; Tiekink, E. R. T.; Young, C. G. *J. Am. Chem. Soc.* **1994**, 116, 9749−9750.

(46) Goodman, J. T.; Inomata, S.; Rauchfuss, T. B. *J. Am. Chem. Soc.* **1996**, *118*, 11674−11675.

(47) Carney, M. J.; Walsh, P, J.; Bergman, R. G. *J. Am. Chem. Soc.* **1990**, *112*, 6426−6428.

(48) de Boer, E. J. M.; de With, J.; Orpen, A. G. *J. Am. Chem. Soc.* **1986**, *108*, 8271−8273.

(49) Gable, K. P.; Phan, T. N. *J. Am. Chem. Soc.* **1994**, *116*, 833−839.

(O)OMe).[14a] In these reactions, the W(VI) oxidation state is retained, in striking contrast to the herein reported reaction of trithio complexes with alkynes. Apparently, terminal thio ligands facilitate reduction of the metal center and thereby allow nonactivated alkynes to form 1,2-enedithiolates.

Concluding Remarks

We have demonstrated that C−S bond cleaving reactions of thiolates offer a convenient synthetic route to a series of mononuclear thio complexes of pentamethylcyclopentadienyl−Mo(VI) and −W(VI), *e.g.*, $Cp^*M(S)_2(S^tBu)$ and $(PPh_4)[Cp^*M(S)_3]$. The reductive C−S bond scission induces oxidation of the metal, which is an advantage of the method because a high metal oxidation state is a requisite for stabilization of mononuclear thio structures. In contrast, most sulfurization reagents, such as alkali metal sulfides, tend to reduce transition metal, and often lead to dinuclear sulfido species. Interestingly the M═S bonds are stable once they are formed. The successful isolation of $[Cp^*M(S)_3]^-$ (M = Mo, W), coupled with the previously reported $[Cp^*M(S)_3]^{2-}$ (M = Nb, Ta), suggests that such half-sandwich trithio complexes of other transition metals might be synthesized. One candidate may be the neutral $Cp^*Re(S)_3$ complex, which is the sulfur analogue of the epoch-making trioxo complex $Cp^*Re(O)_3$.

The M═S bonds of $(PPh_4)[Cp^*M(S)_3]$ (M = Mo, W) are significantly longer than those of the corresponding tetrathiometallates, and the trithio complexes exhibit high reactivity toward alkynes to afford 1,2-enedithiolates, while tetrathiometallates do not react with alkynes. The differing reactivity may arise from the steric bulk and/or electron-donating properties of the Cp* ligand. The reaction with alkynes proceeds very cleanly following second-order kinetics, where the reaction rate is higher for $(PPh_4)[Cp^*Mo(S)_3]$ than its tungsten analog. Transition metal oxo complexes are known to have wide applicability in the oxidation of organic molecules. The facile addition of an alkyne to terminal thio ligands implies the potential use of thio complexes for organic synthesis in the future, and it may provide a convenient entry to an enzyme model relevant to the pterin-containing Mo/W cofactors.

Supporting Information Available: Eyring plots for the reactions of **3** and **11** with diphenylacetylene, tables of atomic coordinates and isotropic thermal parameters, bond distances and angles, hydrogen coordinates, and anisotropic thermal parameters of **3**−**8** and **11**−**13**, and their ORTEP drawings with numbering scheme (88 pages). See any current masthead page for ordering and Internet access instructions.

JA971725E